frontiers | Frontiers in Earth Science

TYPE Review
PUBLISHED 08 March 2023
DOI 10.3389/feart.2023.1047707

OPEN ACCESS

EDITED BY
Fei Xue,
Hohai University, China

REVIEWED BY
Jingcheng Pei,
China University of Geosciences Wuhan, China
Abulimiti Aibai,
Xinjiang Institute of Ecology and Geography (CAS), China
Wen Su,
Institute of Geology and Geophysics (CAS), China

*CORRESPONDENCE
Cun Zhang,
geozhangc@163.com
Fan Yang,
yang_fan1989@126.com

SPECIALTY SECTION
This article was submitted to Structural Geology and Tectonics, a section of the journal Frontiers in Earth Science

RECEIVED 18 September 2022
ACCEPTED 16 February 2023
PUBLISHED 08 March 2023

CITATION
Zhang C, Yang F, Yu X, Liu J, Carranza EJM, Chi J and Zhang P (2023), Spatial-temporal distribution, metallogenic mechanisms and genetic types of nephrite jade deposits in China. *Front. Earth Sci.* 11:1047707. doi: 10.3389/feart.2023.1047707

Spatial-temporal distribution, metallogenic mechanisms and genetic types of nephrite jade deposits in China

Cun Zhang[1]*, Fan Yang[2]*, Xiaoyan Yu[3], Jinhai Liu[1], Emmanuel John M. Carranza[4], Jie Chi[5] and Peng Zhang[1]

[1]School of Materials Science and Engineering, Qilu University of Technology (Shandong Academy of Sciences), Jinan, China, [2]Key Laboratory of Mineral Resources in Western China (Gansu Province), School of Earth Sciences, Lanzhou University, Lanzhou, China, [3]School of Gemology, China University of Geosciences Beijing, Beijing, China, [4]Department of Geology, University of the Free State, Bloemfontein, South Africa, [5]School of Civil and Resource Engineering, University of Science and Technology Beijing, Beijing, China

The nephrite jade deposits of different tectonic units in China exert significant commercial quality, which have attracted wide attention. However, these deposits have not been systematically summarized to date. Here, we investigate the major nephrite jade deposits in China to decipher their gemological and mineralogical characteristics, spatial-temporal distribution, and mineralization processes as well as to identify their geological settings and gemological properties, *via* integrating published geochronology, major and trace elements as well as H-O isotopes. The compiled data suggest that the major nephrite jade deposits in China can also be generally divided into green jade-type (GJ-type) and white jade-type (WJ-type) which covers different species, but most of them belong to the latter. The GJ-type nephrite deposits predominantly occur in ophiolite/ophiolitic mélange suites or are embedded into ultramafic serpentine jade orebodies. This type of nephrite jade mainly formed through the late auto-metamorphic metasomatism of serpentine or the spontaneous crystallization/precipitation along suture/shear zones that acted as pathways to migrate Ca-rich fluids during orogeny. In contrast, the orebodies of WJ-type nephrite jade are usually hosted at the contact zones between the dolomitic marbles and intermediate-felsic or mafic intrusive rocks, which were produced through metamorphism-metasomatism during post continent-continent collision, such as the Kunlun orogenic belt with about ~1,300 km Hetian nephrite belt, and the eastern nephrite jade deposits along the Pacific Ocean. Our study highlights that the nephrite jade deposits in China originally formed during multiple tectonic stages related to the interactions between hydrothermal fluids and metamorphism under subduction accretion- and collision orogenesis-related settings. In addition, this study also provides insights into the genetic discrimination, mineral exploration, and occurrence characteristics of nephrite jade deposits as well as the evaluation and identification of nephrite jade quality.

KEYWORDS

nephrite jade deposits, spatial-temporal distribution, metallogenic mechanism, genetic type, mineral exploration, China

1 Introduction

The nephrite jade, also termed as tremolite jade or Hetian jade in China, is the unique rock reaching the grade of jade and consists mainly of fibrous amphibole (Yu, 2016; Zhang et al., 2021). The amphibole mostly includes tremolite [$Ca_2Mg_5Si_8O_{22}(OH)_2$] and actinolite to ferro-actinolite [$Ca_2(Mg, Fe^{2+})_5Si_8O_{22}(OH)_2$], which usually formed within complex geological processes or different tectonic settings (Figure 1; Yu, 2016; Zhang et al., 2019; Yu et al., 2021). The nephrite jade is characterized by good color, luster, toughness, and transparency and has been regarded as the main carrier of traditional jade culture in China (Yin et al., 2014; Zhang et al., 2019; Zhang et al., 2021). In addition, the nephrite jade also gets continuous attention by Chinese collectors and has occupied a very important role in jade culture or jewelry market (Figures 2A–F).

World-class nephrite jade deposits characterized by economic values are mostly hosted within more than 20 countries and regions (e.g., China, Russia, Canada, America, Poland, Italy, South Korea, New Zealand, and Australia), where more than 120 primary nephrite jade deposits have been excavated in northern and southern zones at different latitudes (Harlow and Sorensen, 2000; 2005; Adams et al., 2007; Kim, 2007; Adamo and Bocchio, 2013; Gao, 2014; Harlow et al., 2014; Qiu, 2016; Gao et al., 2020; Gil et al., 2020; Yu et al., 2021; Feng et al., 2022). Based on the spatial-temporal distribution of global jade deposits, we identified that significant nephrite jade deposits occur along the oceanic coast, cratonic margin, or inland active orogenic belts. In details, these nephrite jade deposits can be summarized into: 1) green nephrites after serpentinization (S-type); and 2) white nephrites after dolomitization (D-type). The former usually developed within/near the global Phanerozoic ophiolite zones and is more abundant than the latter, which could be evidenced by the west and the middle Alps, central Brazil, California, and Alaska extending greenstone belts (Harlow et al., 2014). However, the occurrences of nephrite jade deposits in China are dominated by D-type nephrite jade deposits (Figure 1; Figures 2G, H; Liu et al., 2011a; b, 2015; Gao et al., 2019; Jiang et al., 2021). This may be attributed to the level of excavation or result from the human environment as most Chinese prefer to white nephrite jade, although the majority of ophiolite suites/belts occur throughout the whole China. The nephrite jade species from different regions in China can be effectively distinguished based on the mineral chemistry *via* $Mg^{2+}/(Mg^{2+}+Fe^{2+})$ ratios (Figure 3). Previous investigations have noticed that the nephrite jade in China exerts higher economic value and has larger reserves, which has attracted extensive attention in terms of gemology, mineralogy, and lithology (Harlow et al., 2014; Zhang et al., 2019; 2021; Yu et al., 2021). However, most of these studies only focused on individual localities, ignoring the evaluation on the spatial-temporal characteristics of nephrite jade deposits in China.

Published studies suggested that the S-type nephrite jade deposits are correlated with the Si-rich metasediments that

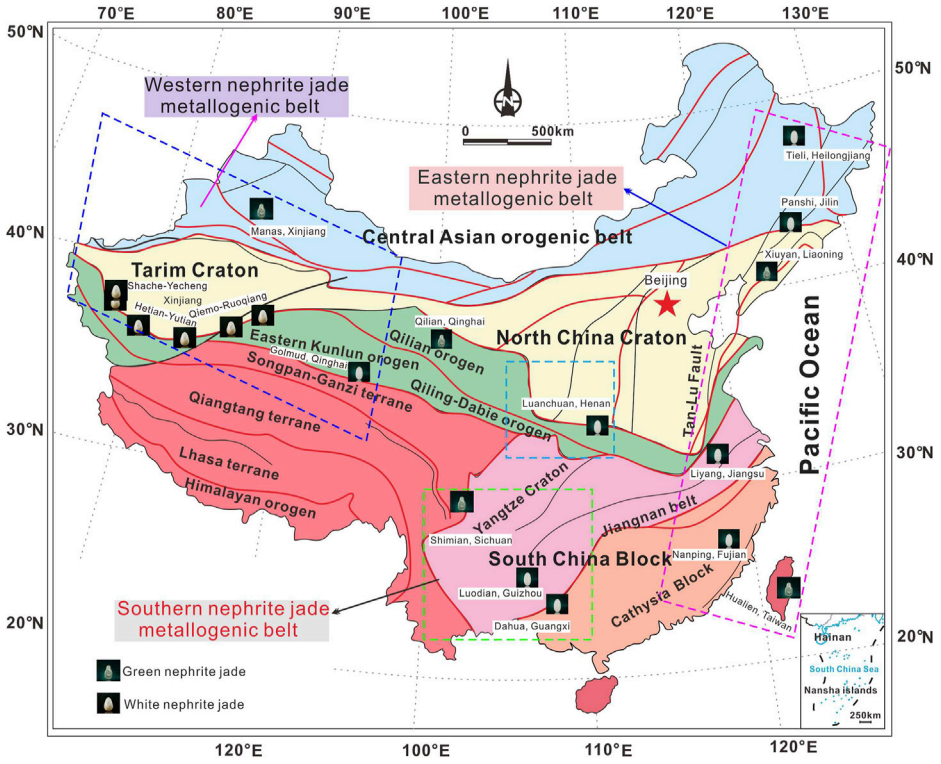

FIGURE 1
Generalized geological and tectonic framework of China, showing different sub-division units (after Qiu et al., 2020; Yu et al., 2021). The major nephrite jade deposits in China are sub-divided into several metallogenic areas, namely, the western nephrite jade metallogenic belt, the eastern nephrite jade metallogenic belt on the west coast of the Pacific Ocean, and the southern nephrite jade metallogenic belt, as well as the central metallogenic belt on the southern margin of North China Craton (NCC), central China, respectively.

FIGURE 2
Representative hand specimen and field photographs. **(A)** The white nephrite jade carving with extremely complex crafts by Yijin Gao (Yu et al., 2021). **(B)** Green nephrite jade from Xiuyan County, Liaoning Province. **(C)** Black placer nephrite jade from the Kalakash River (Black Jade River) shows abundant flaky graphite inclusions. **(D)** White nephrite jade (also named Cuiqing jade) with emerald bands from Qinghai Province. **(E)** Green nephrite jade from Qilian orogenic belts. **(F)** Various colors of nephrite jade from the Gobi Desert. **(G)** D-type nephrite jade deposits showing typical contact between granitoids and dolomitic marble from Yinggelike, Ruoqiang (Jiang et al., 2021). The intrusion of granitoids provided the necessary Si^{4+} and magmatic H_2O, while the old dolomite marble supplied Ca^{2+} and Mg^{2+} during metamorphic-metasomatic processes. **(H)** Nephrite jade open pit from Luchuan, Henan Province. Metagabbro dykes are relatively well developed and emplaced in marbles. And the nephrite ore bodies are generally located in marbles.

interacted with serpentinized mantle peridotite, whereas the D-type nephrite jade deposits are mainly produced by contacting metasomatism between the dolomitic marble and granitic intrusions (Harlow and Sorensen, 2000; 2005; Liu and Yu, 2009; Liu et al., 2011a; 2011b; 2015; Gil et al., 2020; Zhang et al., 2021). These two types of nephrite jade deposits are also widely hosted in China, but which are predominantly related to the serpentine and carbonate bodies, respectively (Liu and Yu, 2009; Yu, 2016; Zhang et al., 2019; Yu et al., 2021; Zhang et al., 2022). However, the formation of nephrite jade deposits is usually controlled by tectonic instability factors that induced the differentials of topographic environments, this further results in the migration and accumulation of source materials, such as Fe, Sr, Si, Ca, Mg, and Cr (Adams et al., 2007; Gil et al., 2020; Zhang et al., 2021; Zhang et al., 2022). Recently, a few studies have correlated the formation environments of S-type nephrite jade with the subduction/obduction–accretionary complex (Yui et al., 2014; Zhang et al., 2021). Based on the investigations of D-type nephrite jade deposit in the Saidikualm, western China, Zhang et al. (2022) identified the formation mechanism of elemental migration variation during nephrite mineralization and also constructed the genetic model of nephrite jade deposits characterized by five mineral assemblage zones. These findings, together with the research outlined by Gao et al. (2019), have theoretically indicated the spatial-temporal variation characteristics of D-type nephrite jade deposits, which also suggested that the formation of nephrite jade deposits was closely correlated with the closure of Proto-Tethys Ocean. Non-etheless, the tectonic evolution for the formation of nephrite jade of these two types of nephrite jade deposits remains unclear, hampering the knowledge of metallogenic mechanisms of nephrite jade deposits.

In this paper, we compiled published studies related to nephrite jade deposits in China, and divided several metallogenic belts of nephrite jade based on their spatial-temporal distributions and variation features, with major aim to provide an overview of detailed characteristics of nephrite jade deposits (Figure 1). In addition, this study also summarizes the gemological properties, geochronological, rare earth elements (REEs), and H-O isotopic features to further probe into the ore genesis of major nephrite jade deposits in China. Further, this study will establish a holistic tectono-metallogenic window in relation to tectonic evolution of the formation of the nephrite jade deposits within subduction/obduction zone or collision orogenic settings.

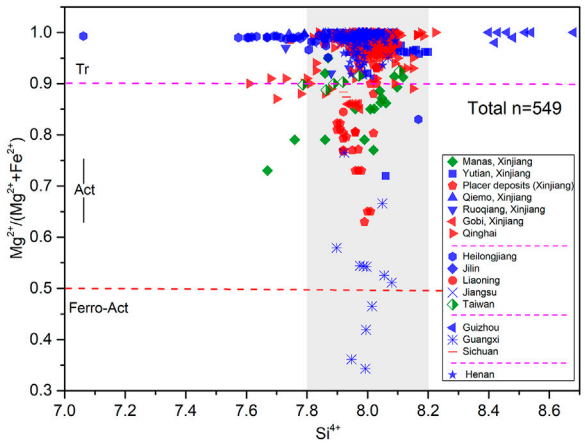

FIGURE 3
The ratios $Mg^{2+}/(Mg^{2+}+Fe^{2+})$ vs. Si^{4+} demonstrate that the nephrite jade is composed of fibrous amphiboles which contain both tremolite and actinolite. The main mineral composition of nephrite jade in China is tremolite, followed by actinolite which is mainly green nephrite and placer nephrite jade, while Ferro-actinolite (black nephrite) is mainly located in Dahua region of Guangxi Province. The contents of Si^{4+} in nephrite are mostly concentrated between 7.8 and 8.2. The contents of Si^{4+} in Luodian nephrite jade are obviously higher than that in other generation areas, while the Tieli nephrite jade from Heilongjiang presents obviously lower content of Si (EMPA Data cited by Liu et al., 2010; 2011; Gao, 2014; Liu et al., 2015; 2016; Yin et al., 2014; Ling et al., 2015; Gao et al., 2019; Bai et al., 2019; Zhong et al., 2019; Zhang et al., 2019; 2021; Jiang et al., 2020; Li et al., 2020; Bai et al., 2020). Tr: tremolite Act: actinolite Ferro-Act: ferro-actinolite.

2 Spatial-temporal distribution of nephrite jade deposits

In China, the S-type nephrite jade deposits are not main jade deposits, which are hosted in Manas, northern slope of Tianshan Mountains of Xinjiang Province (Zhang, 2020). Published studies also suggested that the nephrite jade deposits in China occur predominately in the West Kunlun Orogen along the southern boundary of the Tarim Basin and extend to the northeast of the Altyn Tagh (Figure 1; Liu et al., 2010; 2011; Liu et al., 2015; 2016; Han et al., 2018; Gao et al., 2019; Jiang et al., 2021), which makes up the famous ~1,300 km Hetian nephrite belt and the largest D-type nephrite jade metallogenic belts in the world, although a few D-type nephrite jade deposits formed at different paleo-latitudes within other tectonic units in China. For example, the famous Qinghai nephrite jade deposits distribute along the Hetian nephrite belt extending from southeast to the east of the Kunlun orogenic belt (Lei et al., 2018), but its quality is not as valuable as Xinjiang nephrite jade (Zhang et al., 2019; Zhang et al., 2021). These famous nephrite jade deposits form the western metallogenic belts of nephrite jade in China (Figure 1; Table 1).

In the eastern China, the nephrite jade deposits with different metallogenic scales are distributed along the western Pacific Ocean (Figure 1). Previous studies indicated that these nephrite jade deposits mostly occur in Liaoning (Xiuyan), Jiangsu (Liyang), and Taiwan (Hualien) Province (Figure 1; Table 1; Liao and Zhu, 2005; Zhang et al., 2011; Yin et al., 2014; Yui et al., 2014; Yu, 2016; Zhang et al., 2019; Zhang et al., 2021). With the continuous exploration of nephrite jade deposits, several new nephrite jade deposits have gradually been discovered and are mainly hosted in Heilongjiang (Tieli), Jilin (Panshi), and Fujian (Nanping) Provinces, with small exploration-scales and medium to average jade quality (Table 1; Xu et al., 2014; Gao, 2014; Du, 2015; Ling et al., 2015; Wang et al., 2017; Gao et al., 2019; Bai et al., 2019). Among these, the S-type nephrite jade deposits from Taiwan Province had been confirmed as the youngest nephrite jade deposit on the Earth, which have correlated the metamorphism with the eastward subduction of the South China Sea Plate (Yui et al., 2014). Although these nephrite jade deposits are hosted in the circle-Pacific area as a whole, it is uncertain whether they are related to the subduction of the Pacific plate due to the lack of detailed investigations related to geochronology and tectonic evolution.

In the southern China, the S-type nephrite jade from Shimian County, Sichuan Province shows similar mineralogical characteristics with the Manas S-type nephrite jade (Figure 1; Xu et al., 2015). However, detailed studies on their genesis and tectonic evolution are still lacking at present. Despite the nephrite jade deposits from Guizhou (Luodian) and Guangxi (Dahua) Provinces are all the D-type nephrite jade deposits, their specific genesis and protoliths show quite different characteristics (Figure 1; Yang, 2013; Zhong et al., 2019; Bai et al., 2020). The single metamorphic-hydrothermal metasomatic nephrite jade deposit discovered in Henan (Luanchuan) Province at the southern margin of the North China Craton (Figure 1; Yin, 2006; Ling et al., 2015) can provide significant insights into the tectonic evolution of the North China Craton.

As the valuable jade resources, the nephrite jade deposits can be used as an important proxy to trace geological evolution and non-metallic metallogenic tectonic settings (Zhang et al., 2021). Although the tectonic evolution of these nephrite jade deposits in China are still unclear, based on the spatial-temporal distribution and variation features, we further divided the nephrite jade deposits into four metallogenic belts: 1) the western nephrite jade metallogenic belt, 2) the eastern nephrite jade metallogenic belt along the west coast of the Pacific Ocean, 3) the southern nephrite jade metallogenic belt, and 4) the central nephrite jade metallogenic belt (e.g., Luanchuan nephrite jade deposit at the southern margin of the North China Craton) (Figure 1; Table 1).

3 Genetic types and mineralogy of nephrite jade deposits

The majority of nephrite jade deposits in China are usually correlated with multiple hydrothermal processes (Liu and Yu, 2009). According to the features of ore-forming material sources and fluids differentiation variation, the nephrite jade deposits are divided into the magmatic–hydrothermal metasomatic and metamorphic–hydrothermal metasomatic types. In the following sections, we briefly depict the major characteristics of nephrite jade of each belts. Detailed gemological and mineralogical characteristics of different kinds of nephrite jade were presented in Tables 2, 3.

3.1 Magmatic–hydrothermal metasomatic nephrite jade deposits

All the nephrite jade deposits in the western metallogenic belt are the magmatic–hydrothermal metasomatic type,

TABLE 1 Spatial distributions of major nephrite jade deposits in China.

Provinces		Mineral occurrence	Specific description	Output form	Metallogenic scale prognosis
The western nephrite jade metallogenic belt	Xinjiang	Kunlun Mountain—Altun Mountain ore belts	South of Xinjiang: Shache-Yecheng, Hetian-Yutian, and Qiemo-Ruoqiang metallogenic belts with a total length of ~1,300 km	Primary deposits, primary to secondary/placer deposits, secondary/placer deposits, Gobi nephrite jade	Large scale
		Tianshan Mountain	Northern Xinjiang: the Manas green nephrite jade deposit	Primary deposits, minor secondary or placer deposits	Large scale
	Qinghai	East Kunlun Mountain	Central and western Qinghai: Golmud area	Primary deposits	Large scale
		Qilian orogenic belt	Northeast of Qinghai (including green nephrite jade and serpentine jade)	Primary deposits	Medium to large?
The central nephrite jade metallogenic belt	Henan	Luanchuan County; Tongbai County	West of Henan on the southern margin of the North China Craton	Primary deposits	Medium scale
The eastern nephrite jade metallogenic belt	Heilongjiang	Tieli	Middle of Heilongjiang	Primary deposit	Small scale
	Jilin	Panshi	Central Jilin	Primary deposit	Small scale
	Liaoning	Xiuyan County; Ximu Town	South of Liaoning: Xiyugou (primary jade; placer deposits); Sangpiyu; Ximu jade (placer nephrite jade)	Primary deposits (old jade/primary deposits), Hemo jade (placer type)	Medium to large scale
	Jiangsu	Liyang County	South of Jiangsu (the Meiling jade)	Primary deposit	Medium to small scale
	Fujian	Nanping area	North of Fujian	Primary deposit	Small scale
	Taiwan	Hualien County	East of Taiwan (The Hualien jade)	Primary deposit (green nephrite jade)	Medium scale
The southern nephrite jade metallogenic belt	Sichuan	Western Sichuan region	Shimian County; Wenchuan County	Primary deposits	Medium to small scale
	Guizhou	Luodian County	South of Guizhou (the Luodian jade)	Primary deposit	Medium scale
	Guangxi	Dahua Yao Autonomous County	Central Guangxi	Primary deposit, minor placer or secondary deposit	Medium scale

whereas the majority of nephrite jade deposits in the southern metallogenic belt and few nephrite jade deposits in the eastern metallogenic belt also belong to this genetic type (Figure 2). The nephrite orebodies are controlled by multi-stage fault-fold structures. The hydrothermal fluid were mainly derived from magmatic rocks. It involves the following three sections based on the properties of the intrusion bodies: the ultramafic rock type, the mafic rock type, and the intermediate-felsic rock type (Liu and Yu, 2009).

3.1.1 Ultramafic rock type

The nephrite jade were mainly formed within the ophiolite suites or ophiolite mélange zones, generally featured by green color in its appearance. Their color mainly depends on the content of Fe^{2+} in structure, while Cr^{3+} often plays a marginal role. The protoliths of these deposits can be sourced from a variety of complicated ultramafic complexes, mainly peridotite/serpentinized peridotite and serpentinite with more silicic rocks (Harlow and Sorensen, 2005; Zhang et al., 2021). Representative nephrite jade deposits are mainly discovered in Manas of Xinjiang, Qilian of Qinghai, and Shimian of Sichuan. Details are described below.

3.1.1.1 The Manas green nephrite jade

The jade deposit occurred in the late Paleozoic tectonic belt, which contains carboniferous ophiolite formations with metamorphic peridotite at the bottom, layered gabbro in the middle, and interbedded basalt and siliceous rocks at the top. In details, the orebodies are mainly hosted in Devonian and Carboniferous volcanic rocks and clastic rocks (Tang et al., 2002; Liu and Yu, 2009). The main minerals are featured by tremolite or actinolite with a subordinate association of diopside, chromite, chlorite, serpentine, talc, and sulfide, arsenide of nickel. Published mineral major element data suggested that the main chemical compositions of amphibole in the western section of the nephrite jade deposit are the SiO_2 (59.12–54.89 wt%), MgO (13.50–10.99 wt %), CaO (25.85–20.47 wt%), and FeO (6.25–1.94 wt%; average value: 3.19 wt%). In contrast, the main chemical compositions of SiO_2, MgO, CaO in the eastern section of the deposit vary from 57.97 to 59.23 wt%, 12.48–13.00 wt%, 20.28–21.93 wt%, and 3.57–6.31wt%, respectively. Together, these suggest that the S-type nephrite jade in the western section of this deposit is tremolite, whereas the eastern section of this deposits is actinolite (Tian, 2014; Zhang, 2020). In addition, the H-O isotopic data show that the $\delta^{18}D_{H2O}$ values range from −76.7‰ to −5.8‰; while the $\delta^{18}O_{H2O}$ values range from 9.8‰ to 12.6‰, respectively (Figure 5; Zhang, 2020).

TABLE 2 Overview of the gemological and mineralogical characteristics of nephrite jade deposits in China.

Magmatic-hydrothermal metasomatic nephrite							
Genetic type	Ultramafic rock type			Mafic rock type			References
Locations	Manas, Xinjiang	Shimian, Sichuan	Qilian, Qinghai	Golmud, Qinghai	Luodian, Guizhou	Dahua, Guangxi	
Color	Green, dark green, light green, and yellow jade	Light green, dark green, brown, gray, dark gray, and yellow jade	Green, dark green, and black green jade	White, light greenish white, greenish, green, emerald, and brown jade	White, gray, yellow white, light green, gray green, and brown jade	White, gray, light green, gray green, and black jade	Zhi et al. (2011); Du (2015); Zhang et al. (2021); Bai et al. (2020)
Texture and transparency	Fine texture; microtransparent—opaque	Relatively fine texture; translucent—opaque	Translucent—opaque	Fine texture; microtransparent—translucent	Fine texture; microtransparent—opaque	Fine texture; microtransparent—opaque	Du (2015); Zhang et al. (2021)
Luster	Vitreous—greasy luster	Vitreous luster	Vitreous luster	Weak greasy luster—vitreous luster	Waxy—weak greasy luster	Waxy—weak greasy luster	
Refractive index	1.60-1.61	1.60–1.62	1.60	1.61-1.62, the average: 1.612	1.60–1.62	1.60–1.62	Zhou et al. (2008); Ding (2011); Zhang (2013); Tian (2014); Du (2015); Zhang et al. (2021)
Specific gravity	The average value: 2.97	2.91–3.01	2.95–2.97	2.94–3.06; The average: 2.97	The average value: 2.86-2.87	The average: 2.94	Zhou et al. (2008); Ding (2011); Zhang (2013); Tian (2014); Du (2015); Zhang et al. (2021)
Hardness (Mohs hardness)	6.0–6.5	5.5–6.0	5.5–6.0	The average value: 5.57	6.0–7.0	The average value: 5.70	Ding (2011); Zhang (2013); Du (2015)
Chelsea filter	No change	No change	No change	No change	No change	No change	
Ultraviolet fluorescence	Inertia, related to the content of Fe	Inertia	Inertia	Inertia	Inertia	Inertia	
Spectroscopy characteristics	FTIR: 3,800–3,600 cm^{-1}, 1,200–900 cm^{-1}, 800–600 cm^{-1}, 600–400 cm^{-1}; laser Raman: 3,674 cm^{-1}, 1,060 cm^{-1}, 670 cm^{-1}, 220 cm^{-1}	FTIR: 3,700–3,600 cm^{-1}, 1,100–960 cm^{-1}, 800–600 cm^{-1}, 600–400 cm^{-1}; laser Raman: 1,060 cm^{-1}, 1,030 cm^{-1}, 675 cm^{-1}	FTIR: 1930 cm^{-1}, 1,058 cm^{-1}, 950–920 cm^{-1}, 671 cm^{-1}, 528 cm^{-1}, 505 cm^{-1}, 415 cm^{-1}, 220 cm^{-1}	FTIR: 1,200–900 cm^{-1}, 760–640 cm^{-1}, 550–400 cm^{-1}; laser Raman: 1,056 cm^{-1}, 674 cm^{-1}, 219 cm^{-1}	FTIR: 3,750–3,550 cm^{-1}, 1,200–800 cm^{-1}, 600–400 cm^{-1}	FTIR: 3,700–3,500 cm^{-1}, 1,200–800 cm^{-1}, 800–600 cm^{-1}, 600–400 cm^{-1}; laser Raman: 1,056 cm^{-1}, 674 cm^{-1}, 219 cm^{-1}	Lu et al. (2004); Lu, 2005, 2007, 2008; Yang, et al., 2013, Yang, 2013; Tian (2014); Du (2015); Song et al. (2020); Zhang (2020)
Micro-examination	Fibrous, columnar, acicular, flake and irregular	Tremolite grains extend in a directional fibrous orientation	Tremolite grains present fibrous, columnar, and flaky forms	Tremolite grains show microfibrous, flake and radial forms. The aggregate morphologies include cryptocrystalline aggregates, astatic fiber aggregates, near parallel fiber bundle, and radial fiber cluster	Tremolite grains are mainly fibrous, acicular and scaly	Tremolite grains are mainly acicular, fibrous and columnar	Feng and Zhang (2004)

(Continued on following page)

10.3389/feart.2023.1047707

TABLE 2 (*Continued*) Overview of the gemological and mineralogical characteristics of nephrite jade deposits in China.

Magmatic-hydrothermal metasomatic nephrite							
Genetic type	Ultramafic rock type			Mafic rock type			References
Locations	Manas, Xinjiang	Shimian, Sichuan	Qilian, Qinghai	Golmud, Qinghai	Luodian, Guizhou	Dahua, Guangxi	
Textures	Granulitic crystalloblastic texture, heteroblastic texture, microcrystalline crystalloblastic texture, metasomatism structure	Microfiber crystalloblastic texture, Microscopic porphyritic crystalloblastic texture, with occasionally metasomatism harbour - like structure	Fiber interwoven texture, fiber crystalloblastic texture, metasomatic pseudomorph texture, broom texture, metasomatic rim texture	Felt-like texture, microfiber-cryptocrystalline texture, microflake—cryptocrystalline texture, microflake texture, radial fiber structure, secondary filling texture, metasomatic pseudomorph texture	Felt-like fiber interwoven crystalloblastic texture, fiber interwoven crystalloblastic texture, fiber bundle-crystalloblastic texture, lepidoblastic texture, metasomatic relict texture	Microfiber crystalloblastic Texture, felted fibrous crystalloblastic texture, metasomatic relict texture	Feng and Zhang (2004); Zhou et al. (2008); Qin (2013); Zhang (2013); Du (2015); Yu (2016); Bai et al. (2020)
Structures	Massive	Massive	Massive	Massive and band structure	Massive, flaky, and banded structure	Massive	
Cleavage or fracture	Uneven fracture	Uneven fracture	Uneven fracture	Uneven fracture	Uneven fracture	Uneven fracture	
Major mineral	Tremolite/actinolite	Tremolite/actinolite	Tremolite/actinolite	Tremolite	Tremolite	Tremolite	
Secondary or accessory minerals	Diopside, chromite, chlorite, serpentine, talc, and sulfide, arsenide of nickel	Titanite, chlorite, magnetite, calcite, serpentine, etc.	Actinolite, apatite, chlorite, titanite	Apatite, pyrite, actinite, diopside, titanite, magnetite, chromite (green jade), epidote, dolomite, calcite, quartz, clay minerals, etc. Black jade usually contains graphite, magnetite, and ilmenite	Diopside, albitite, calcite, quartz, moganite, dolomite, apatite, ferromanganese or clay minerals	Diapsite, calcite, chlorite, quartz, apatite, titanite, andradite, talc; stilpnomelane, epidote, diopside, pyrrhotite, and pyrite (black jade)	Lu et al. (2004); Zhou, et al. (2008); Ding (2011); Tang et al. (2002); Qin, Y. (2013); Yang (2013); Zhang (2013); Che (2013); Du (2015); Dong et al. (2014); Zhang (2015); Zhong et al. (2019); Zhang et al. (2021); Lan (2022)

Genetic type	Intermediate-felsic rock type						
Locations	Yutian, Xinjiang	Hetian, Xinjiang	Qiemo, Xinjiang	Ruoqiang, Xinjiang	Gobi nephrite jade, Xinjiang	Liyang, Jiangsu	References
Color	White jade, light greenish white jade, greenish jade, black jade, and brown jade	White jade, greenish jade, black jade, and yellow jade	White jade, light greenish white jade, greenish jade, and brown jade	greenish jade, light greenish white jade, brown jade, and yellow jade	White jade, light greenish white jade, yellowish jade, light brown jade	White jade, light greenish white jade, greenish jade, and green jade	Yu (2016); Wu (2016)

(Continued on following page)

10.3389/feart.2023.1047707

TABLE 2 (*Continued*) Overview of the gemological and mineralogical characteristics of nephrite jade deposits in China.

Genetic type	Intermediate-felsic rock type						
Locations	Yutian, Xinjiang	Hetian, Xinjiang	Qiemo, Xinjiang	Ruoqiang, Xinjiang	Gobi nephrite jade, Xinjiang	Liyang, Jiangsu	References
Texture and transparency	Fine texture; microtransparent—opaque	Fine texture; microtransparent—opaque	Fine texture; microtransparent—opaque	Fine texture; microtransparent—opaque	Fine texture; microtransparent—opaque	Coarse textures; microtransparent—opaque	Yu (2016); Wu (2016)
Luster	Greasy luster	Greasy luster	Vitreousr-greasy luster	Vitreous-greasy luster	Strong greasy luster	Semi-greasy luster	Yu (2016); Wu (2016)
Refractive index	1.60-1.61	1.60-1.61	1.60	1.60–1.62	1.61–1.62	1.60	Li and Cai (2008); Yu (2016); Wu (2016)
Specific gravity	2.95±	The average value: 2.97	2.94–2.98	2.90–3.00	The average value: 2.97; slightly higher than that of primary deposits	The average value: 2.95–2.99	Zhong (1995); Li and Cai (2008); Zhou et al. (2009); Yu (2016); Qiu (2016); Wu (2016); Su et al. (2019)
Hardness (microhardness or Mohs hardness)	The Mohs hardness: 6–6.5	The Mohs hardness: 6.0–6.5	The Mohs hardness: 6.14–6.41, with an average of 6.29	The Mohs hardness: 5.80–6.10	The Mohs hardness: 6.23–6.24	5.5–6.0	Zhong (1995); Yu (2016); Qiu (2016); Wu (2016); Su et al. (2019)
Chelsea filter	No change	No change	No change	No change	No change	No change	
Ultraviolet fluorescence	Inertia	Inertia	Inertia	Inertia	Inertia	Inertia	
Spectroscopy characteristics	FTIR: 1,144–915 cm^{-1}, 758–640 cm^{-1}, 544–460 cm^{-1}	FTIR: 1,100–900 cm^{-1}, 900–600 cm^{-1}, 600–400 cm^{-1}; laser Raman: 3,676 cm^{-1}, 1,060 cm^{-1}, 930 cm^{-1}, 672 cm^{-1}, 395 cm^{-1}, 223 cm^{-1}	FTIR: 1,100–900 cm^{-1}, 800–600 cm^{-1}, 600–400 cm^{-1}; laser Raman: 3,676 cm^{-1}, 677 cm^{-1}, 226 cm^{-1}	FTIR: 3,700–3,600 cm^{-1}, 1,200–900 cm^{-1}, 550–400 cm^{-1}, 800–650 cm^{-1}; Laser Raman: 1,058 cm^{-1}, 675 cm^{-1}, 223 cm^{-1}	FTIR: 1,150–900 cm^{-1}, 760–400 cm^{-1}; laser Raman: 3,672 cm^{-1}, 1,061 cm^{-1}, 225 cm^{-1}	FTIR: 1,100–900 cm^{-1}, 760–400 cm^{-1}, 400–200 cm^{-1}	Zou et al. (2002); Cui and Yang (2002); Yang et al. (2012); Zhang et al. (2012); Chen et al. (2013); Qiu (2016); Wu (2016); Su et al. (2019)
Micro-examination	Tremolite grains are irregular fibrous or columnar, and fibrous tremolite extends semi—directionally, and some areas are intertwined and closely bound together; Some grains show radial or fascicular structures	Tremolite grains are very fine without distinct boundaries, and they are intertwined and closely bound together; Some tremolite grains show radial or fascicular structures	Tremolite grains are irregular fibrous or columnar, and the fibrous tremolite generally extends semi—directionally, and some areas are intertwined and closely bound together	Most of the tremolite grains are fibrous, a few tremolite grains are distributed in fibrous tremolite in columnar or granular forms	Tremolite grains are arranged in felt-like and columnar orientation	Tremolite grains commonly present fibrous, needle-like, columnar, lamellar, radial forms	Liu et al. (2015); Qiu (2016); Wu (2016); Gao et al. (2019)

(Continued on following page)

10.3389/feart.2023.1047707

TABLE 2 (*Continued*) Overview of the gemological and mineralogical characteristics of nephrite jade deposits in China.

Genetic type	Intermediate-felsic rock type						
Locations	Yutian, Xinjiang	Hetian, Xinjiang	Qiemo, Xinjiang	Ruoqiang, Xinjiang	Gobi nephrite jade, Xinjiang	Liyang, Jiangsu	References
Textures	Felt-like fiber interwoven texture, microfiber-cryptocrystalline, microfiber, microflake cryptocrystalline, microflake metamorphosis and radial or broom texture, with occasionally metasomatism residual texture	Felt-like fiber interwoven texture, fiber interwoven—crystalloblastic texture	Felt-like fiber interwoven texture, microacicular—crystalloblastic texture, columnar—crystalloblastic texture, heteroblastic—crystalloblastic textureetc	Felt-like fiber interwoven texture, microfiber-cryptocrystalline crystalloblastic texture, microfiber crystalloblastic texture, broom texture, fiber bundle texture, porphyroblastic texture, metasomatic pseudomorph texture, metasomatism residual texture, secondary filling texture	Felt-like interwoven texture, microfiber crystalloblastic texture	Felt-like structure, radial texture, fiber-columnar texture	Cui and Yang (2002); Liu et al., 2011; Meng, 2014; Liu et al. (2015); Qiu (2016)
Structures	Massive structure with occasionally flake structure	Massive structure	Massive structure	Massive structure	Flake/massive structure	Massive structure	
Cleavage or fracture	Uneven fracture	Uneven fracture	Uneven fracture	Uneven fracture	Uneven fracture	Uneven fracture	
Major mineral	Tremolite (>98%)	Tremolite (>98%)	Tremolite (>98%)	Tremolite	Tremolite/actinolite (green nephrite jade)	Tremolite/actinolite	
Secondary or accessory minerals	Diopside, chlorite, phlogopite, calcite, dolomite, titanite, biotite	Diopside, actinolite, graphite, apatite, allanite, grossularite, zircon, and rutile	Diopside, dolomite, titanite, epidote, magnetite, apatite, limonite, zoisite, chlorite	Pargasite, diopside, epidote, allanite, titanite, andesine, prehnite, calcite	Apatite, titanite, diopside, epidote, chromite (green jade), feldspar, pyrope	Diopside, muscovite, epidote, pyroxene, apatite, magnetite, limonite, clay minerals	Cui and Yang (2002); Zhou et al. (2009); Liu et al., 2010, 2011; Liu et al. (2015); Qiu (2016); Wang (2016); Wu (2016); Gao et al. (2019); Liu et al. (2019)

10.3389/feart.2023.1047707

TABLE 3 Overview of the gemological mineralogical characteristics of nephrite jade deposits in China.

Genetic type	Serpentine rock type	Carbonate rock type		References
Locations	Hualien, Taiwan	Xiuyan, Liaoning	Luanchuan, Henan	
Color	Chartreuse, dark green, bright green, grass green and other green with light yellow and light white jade; Nephrite jade with cat's effect usually show yellow with green, black or brown color	Light greenish white, chartreuse, black green, and dark green jade	White, light greenish white, azury jade	
Texture and transparency	Fine texture; Microtransparent—opaque	Medium - fine texture; Translucent—opaque	Medium—fine texture; Opaque	Ding (2011); Zhang et al. (2019)
Luster	Waxy—greasy luster	Vitreous luster	Waxy luster	Zhang et al. (2019)
Refractive index	1.61–1.63	1.60–1.61	1.60 ± 0.02	Zhang et al. (2019)
Specific gravity	3.02–3.44	2.85–2.96	2.95 ± 0.01	Zhang et al. (2019)
Hardness (microhardness or Mohs hardness)	The Mohs hardness: 5–6	5.90–6.57	—	Zhang et al. (2019)
Chelsea filter	No change	No change	No change	Zhang et al. (2019)
Ultraviolet fluorescence	Inertia related to the content of Fe	Inertia	Inertia	Zhang et al. (2019)
Spectroscopy characteristics	FTIR: 3,700–3,600 cm^{-1}, 1,200–900 cm^{-1}, 600–400 cm^{-1}, 800–600 cm^{-1}; laser Raman: 1,056 cm^{-1}, 671 cm^{-1}, 218 cm^{-1}	FTIR: 1,200–900 cm^{-1}, 600–400 cm^{-1}, 800–600 cm^{-1}; laser Raman: 1,060 cm^{-1}, 1,030 cm^{-1}, 670 cm^{-1}	—	Ding (2011); Li et al. (2011); Ren et al. (2012); Chen, et al. (2013); Zhang et al. (2019)
Micro-examination	Columnar, microfibrous (astatic, parallel, nearly parallel, bunched shapes)	Tremolite grains usually show tabular, columnar, foliaceous and fibrous foem, and generally contain abundant graphite inclusions	Tremolite grains show microfibrous, lamellar forms etc.	Zhang et al. (2019)
Textures	Felt-like crystalloblastic texture, columnar crystalloblastic texture, parallel fiber crystalloblastic texture, metasomatic pseudomorph texture	Felt-like interwoven texture, microfiber crystalloblastic texture, micro-radial (broom) texture, micro leaf-like—crystalloblastic texture	Felt-like fiber interwoven metamorphosis texture, Fiber bundle crystalloblastic texture, radial crystalloblastic texture, porphyritic—crystalloblastic is texture, rotational texture, metasomatic relict texture, etc.	Ding (2011); Li et al. (2011); Ren et al. (2012); Lin (1999); Zhang et al. (2019)
Structures	Massive structure	Massive structure	Massive structure	Tang et al. (2002); Yin (2006); Ling et al. (2008); Ding (2011); Zhang et al. (2019)
Cleavage or fracture	Uneven fracture	Uneven fracture	Uneven fracture	Tang et al. (2002); Ding (2011); Zhang et al. (2019)
Major mineral	Tremolite/actinolite	Tremolite	Tremolite	Tang et al. (2002); Ding (2011); Zhang et al. (2019)
Secondary or accessory minerals	Actinolite, chromite, chromium-bearing essonite, magnetite, titanite, serpentine, chlorite, and graphite	Serpentine, calcite, dolomite, titanite, zoisite, apatite, and graphite	Calcite, titanite, rutile, quartz, serpentine, actinolite, chlorite, pyrite, apatite, magnetite	Tang et al. (2002); Yin (2006); Ding (2011); Li et al. (2011); Liao et al. (2012); Ren et al. (2012); Ling et al. (2015); Zhang et al. (2019)

3.1.1.2 The Qilian green nephrite jade

The jade mainly formed within the North Qilian orogenic belt, but there are still shortage of studies to investigate them (Zhang et al., 2021). A previous investigation suggested that the high-quality S-type nephrite jade in Yushigou region, the Qilian Orogen is predominantly composed of tremolite and actinolite, and underwent the transformation to actinolite with the increasing of Fe and Cr (Zhang et al., 2021). The secondary or accessory minerals consist of apatite, chlorite, and titanite. Usually, the green nephrite jade shows two different colors: deep green and greyish-green, characterized by delicate textures and vitreous luster (Figure 1, Figure 2E). The major element data suggest that the mineral chemical compositions of tremolite are main SiO_2 (55.90–59.04 wt%), MgO (20.36–22.29 wt%), CaO (12.62–13.24 wt%) and FeO (3.47–5.48 wt%) (Zhang et al., 2021).

3.1.1.3 The Shimian green nephrite jade

The jade deposit hosted in Sichuan Province is famous for producing high-quality nephrite with chatoyancy (Xu et al., 2015). The ore-bearing rock masses are mainly serpentinized augite peridotite and peridotite intruding in the middle Proterozoic Ebian Group. Due to uniform directional shear stress during metasomatism, tremolite fibers, needle-like minerals or tubular gas-liquid inclusions were orientated growth, which led to the formation of nephrite jade with the cat's eye effect (Xu et al., 2015). The main minerals of the nephrite jade are characterized by fibrous tremolite or actinolite, together with minor titanite, magnetite, and serpentine, and the major chemical compositions of tremolite are SiO_2 (56.85–57.27 wt%), MgO (21.61–22.99 wt%), CaO (12.29–13.13 wt%), and FeO (up to 5.60 wt%) (Lu, 2005; Ding, 2011; Xu et al., 2015).

3.1.2 Mafic rock type

The nephrite jade orebodies occurred within the contact zones between the dolomitic marbles and mafic intrusive rocks. Most of orebodies are distributed along faults or cracks of dolomitic marble and occur as layers, veins or lenses. Representative nephrite jade deposits are mainly distributed in Sanchakou of Qinghai, Luodian of Guizhou and Dahua of Guangxi. Details are as follows.

3.1.2.1 The Sanchakou nephrite jade

The jade deposit is located in the north of Kunnan fault zone and the south of Kunzhong suture zone, and the nephrite jade of this deposit generally shows characteristics of high hardness, low tremolite content, and high crystallinity (Zhou et al., 2005). The igneous rocks exposed in this ore district are mainly mafic gabbro (Ma, 2013), while the jade ore intrusive body is dioritic porphyrite. The nephrite formation was accompanied by multiple hydrothermal fluids reactions during the mineralization processes.

3.1.2.2 The Luodian nephrite jade

The nephrite jade (also termed as Luodian jade) from Guizhou Province, a new genetic type of jade variety, represents an important part of Chinese nephrite jade (Yang, 2013). The occurrences and mineralization of Luodian jade predominantly occur at contact metamorphic zones, whereas the distribution of it was strictly controlled by anticlinal structure and diabase emplacement (Che, 2013; Zhang, 2013; Zhang, 2015). The Luodian jade consists mainly of white jade, white-green jade, and green jade. The green nephrite jade is caused mainly by trace elements of V and Cr in chemical compositions (Yang, 2013). The main minerals include tremolite as well as minor diopside, calcite, quartz, wollastonite, plagioclase, and talc.

3.1.2.3 The Dahua nephrite jade

The jade deposit (also termed as Dahua jade) located Guangxi occurs in alteration zones of marble overlying diabase, presenting the characteristics of strata-bound ore deposit (Lan, 2022). The major minerals are characterized by fibrous tremolite with a subordinate association of diapsite, calcite, chlorite, quartz, apatite, titanite, and andradite, and talc (Du, 2015; Lan, 2022). Recent published mineral major element data suggested that the main chemical compositions of tremolite in the nephrite jade are the SiO_2 (the average value 59.31 wt%), MgO (the average value 23.63 wt%), CaO (the average value 12.99 wt%) (Lan, 2022). However, the black nephrite jade with high quality consists mainly of actinolite or ferro-actinolite, together with minor stilpnomelane, andradite, patite, epidote, quartz, diopside, pyrrhotite, and pyrite, with a $Mg/(Mg^{2+} + Fe^{2+})$ ratio of 0.765–0.343 (Figure 3; Zhong et al., 2019).

3.1.3 Intermediate-felsic rock type

The primary orebodies of these nephrite jade deposits generally occur at the contact zones between the dolomitic marbles and intermediate-felsic rocks (generally granitoids). The lithologies of these deposit are mainly composed of a suite of calcium–magnesian marbles. Most of orebodies are also distributed along faults or cracks of dolomitic marble and occur as veins or lenses. About 20 nephrite jade deposits are discovered in the Kunlun Mountain, and they are concentrated in several regions: Shache-Yecheng belt, Hetian-Yutian belt, and Qiemo-Ruoqiang belt (Liu et al., 2010; 2011; Liu et al., 2015; 2016; Han et al., 2018; Gao et al., 2019; Jiang et al., 2021). In the following sections, we also briefly introduce the major features of representative nephrite jade of each belts in the order described above.

3.1.3.1 The placer/secondary nephrite jade

The jade deposits are mainly distributed in two tributaries of the Yurungkash River (White Jade River) and Kalakash River (Black Jade River) in Hetian County (Liu et al., 2011; 2016). This kind of nephrite jade was transported by glacial melt-water, and deposited into river (or bed) from the primary deposits in the Kunlun Mountains (Liu et al., 2016). In this mining area, the black nephrite jade can be divided into two types: 1) jade dominated by tremolite and actinolite; and 2) jade with tremolite and graphite (Figure 2C). The nephrite jade generally shows low ΣREE contents, and whole-rock chondrite standardized data display that this nephrite jade has strong negative Eu anomalies, moderate light-REEs enrichments, and flat heavy-REE enrichments (Liu et al., 2011; 2016) (Figure 4A). Moreover, H-O stable isotopes of the nephrite jade ($\delta^{18}D_{H2O}$: −86.1‰–−5.8‰; $\delta^{18}O_{H2O}$: 1.5‰–8.4‰) indicated that the nephrite jade formation is related to carbonate bodies (Liu et al., 2016), but not to serpentinite. SHRIMP zircon U–Pb dating for black nephrite jade yielded $^{206}Pb/^{238}U$ mean ages of 440.7 ± 4.4 Ma, 397.1 ± 3.5, and 389 ± 4 Ma, and of 377.8 ± 6.2 Ma for white-green nephrite jade (Liu et al., 2016) (Figure 6).

3.1.3.2 The Alamas nephrite jade

The jade deposit located in Yutian region was characterized by strong tectonic movement and extensive thrust faults in late Hercynian period. The main minerals are featured by tremolite with a subordinate association of diopside, chlorite, calcite, titanite, and phlogopite. The jade deposit is mainly hosted the contents of tremolite are MgO, CaO and SiO_2, ranging from 18.89 to 26.55 wt%, 10.20–12.67 wt%, and 53.25–58.58 wt% (Liu et al., 2010), respectively. The Alamas nephrite jade also has pronounced Eu negative anomalies (δEu = 0.08–0.17), characterized by depleted in LREEs and flat HREEs in the chondrite-normalized patterns (Liu et al., 2015) (Figure 4A). Nephrites have $\delta^{18}O_{H2O}$ and $\delta^{18}D_{H2O}$ isotope compositions in the range from 3.4‰ to 6.1‰ and −73.0‰ to −61.3‰, respectively (Figure 5). Zircon U–Pb geochronology of granodiorite reveals the age of magmatic zircons was at 418.5 ±

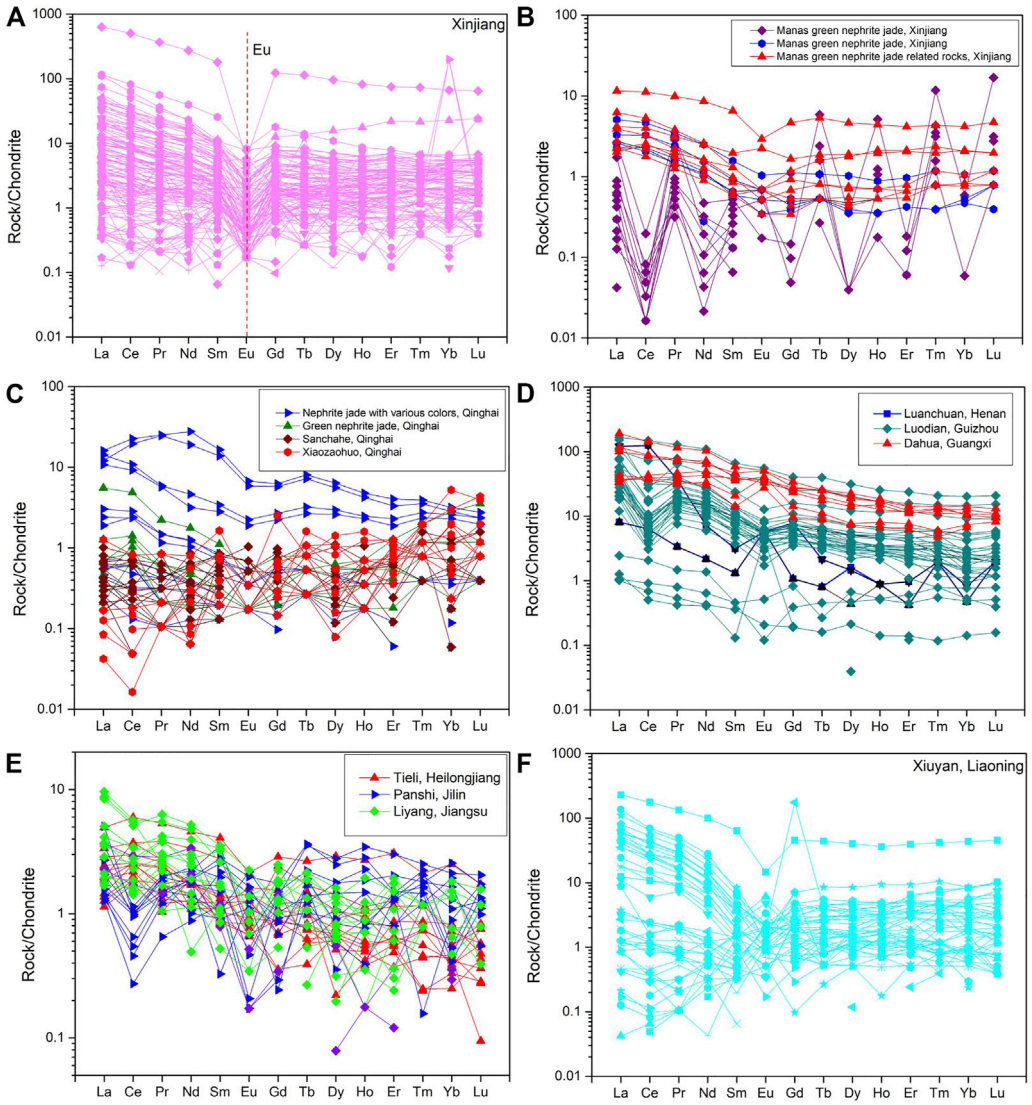

FIGURE 4
The Chondrite-normalized REE patterns of nephrite jade from Xinjiang **(A,B)**, Qinghai **(C)**, Henan **(D)**, Guizhou **(D)**, Guangxi **(D)**, Heilongjiang **(E)**, Jilin **(E)**, Jiangsu **(E)**, as well as Liaoning **(F)**, respectively. The chondrite-normalized values are from McDonough and Sun (1995). Nephrite jade in different regions shows obviously disparate variation of REEs, indicating the distinction of the regularity of ore formation process (Data cited by Ling et al., 2008; Li et al., 2011; Zhi et al., 2011; Yang, 2013; Gao, 2014; Zhang, 2015; Liu et al., 2015; 2016; Yin et al., 2014; Ling et al., 2015; Yu, 2016; Li, 2016; Liu et al., 2019; Gao et al., 2019; Bai et al., 2019; Jiang et al., 2020; Bai et al., 2020).

2.8 Ma, constraining the upper limit age of nephrite jade formation (Liu et al., 2010; 2015) (Figure 6).

3.1.3.3 The Tashsaii nephrite jade

The deposit in the southwest of the Altyn Tagh Fault are mainly hosted in the Qiemo County (Gao et al., 2019). Currently, it is the largest nephrite jade deposit in the Xinjiang Province, including Jinshan, Tiantai, and 8th mine open pits (Gao et al., 2019). Wu (2016) proposed that the dolomite marble was generally characterized by white tremolitization, yellow-green serpentinization, and pink zoisitization. The main minerals are featured by tremolite with a subordinate association of diopside, dolomite, titanite, epidote, magnetite, apatite, limonite, zoisite, chlorite. The predominant mineral of the Tashsaii nephrite jade is tremolite, and its mineral chemical compositions show MgO contents of 23.46–26.01 wt%, CaO contents of 10.87–14.06 wt%, and SiO_2 contents of 57.23–59.50 wt% (Wu, 2016; Gao et al., 2019). The Tashsaii nephrite jade displays enrichment in LREEs and depletion in HREEs (Figure 4A). Zircon U–Pb dating of zoisite-quartz altered rocks constrains that the nephrite jade from this region was formed at 433 ± 10 Ma (Gao et al., 2019) (Figure 6).

3.1.3.4 The Yinggelike and Fuguoling nephrite jade

The jade deposits in the mining area are mainly distributed in Ruoqiang region, among which the Yinggelike nephrite jade generally presents yellow color. The main minerals of nephrite jade are featured by tremolite with a subordinate association of Pargasite, diopside, epidote, allanite, titanite, andesine, prehnite, and calcite (Jiang et al., 2020). Their mineral chemistry compositions of SiO_2, MgO and CaO vary from 56.96 to 59.74 wt%, 21.05–24.07 wt

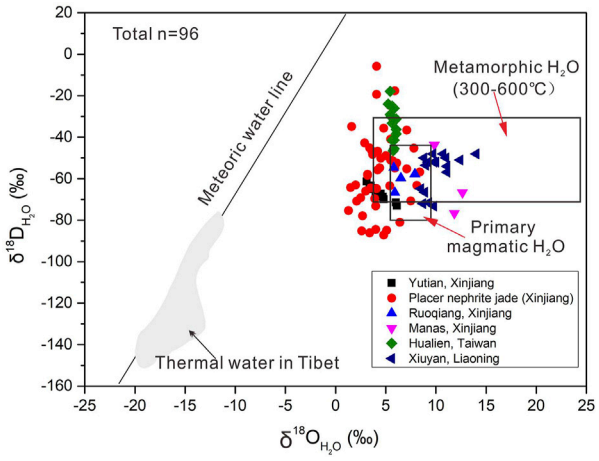

FIGURE 5
δD_{H2O} and $\delta^{18}O_{H2O}$ data for ore-forming fluids of representative nephrites from different regions. The diagram is from Taylor (1997), showing the evolution of hydrothermal fluids (Liu et al., 2011; 2016). The Magmatic water, metamorphic water, together with minor meteoric water were involved to participate in the formation process and evolution of nephrite jade in China (Data cited by Liu et al., 2011; 2015; 2016; Zheng et al., 2019; Jiang, 2020; Zhang, 2020; Gao et al., 2020).

%, and 12.77–13.89 wt%, respectively. The contents of Fe^{3+} and Fe^{2+} are the main factors to control the color of nephrite jade. The REEs distribution patterns and H-O stable isotopic of the Yinggelike nephrite jade ($\delta^{18}D_{H2O}$: −66.7‰ to −54.6‰; $\delta^{18}O_{H2O}$: 5.8‰–7.9‰) indicate a genetic link with dolomite marble (Figure 4A, Figure 6). In contrast, the contents of SiO_2, MgO and CaO in the Fuguoling nephrite jade show variation range of 56.01–58.96 wt%, 21.43–24.14 wt%, and 12.07–14.02 wt%, respectively. Zircon U–Pb dating of granite constrains the upper limit age of tremolite crystallization at 471 ± 16 Ma (Figure 6; Jiang, 2020).

3.1.3.5 The Gobi nephrite jade

The jade is widely hosted in the Qiemo-Ruoqiang County, characterized by certain edges and corners, as well as with strong greasy luster (Fang, 2018). The main minerals of the Gobi nephrite jade is tremolite, and its main mineral chemical compositions of SiO_2, MgO, and CaO range from 56.7 to 58.9 wt%, 23.6–24.8 wt%, and 12.16–15.0 wt% (Liu et al., 2019; Su et al., 2019), respectively. The secondary or accessory minerals consist of apatite, titanite, diopside, epidote, feldspar, and pyrope. In terms of the REEs distribution patterns, the Gobi nephrite has obvious Eu negative anomalies, similar with primary nephrite jade (Figure 4A). Liu et al. (2019) studied trace elements, and REEs of the Gobi nephrite jade from Ruoqiang–Qiemo areas, and concluded that the nephrite jade is correlated with magnesium skarn type (Figure 5). Moreover, SHRIMP zircon U–Pb dating of the nephrite jade yielded $^{206}Pb/^{238}U$ mean ages of ca. 400 Ma, which constrain the formation of the Gobi nephrite jade. Other zircon U-Pb ages of 2,460–1,450 Ma, 785 Ma, and 60–40 Ma may represent new zircon growth, magmatic hydrothermal events, and protolithic sedimentary ages (Liu et al., 2019) (Figure 6), respectively.

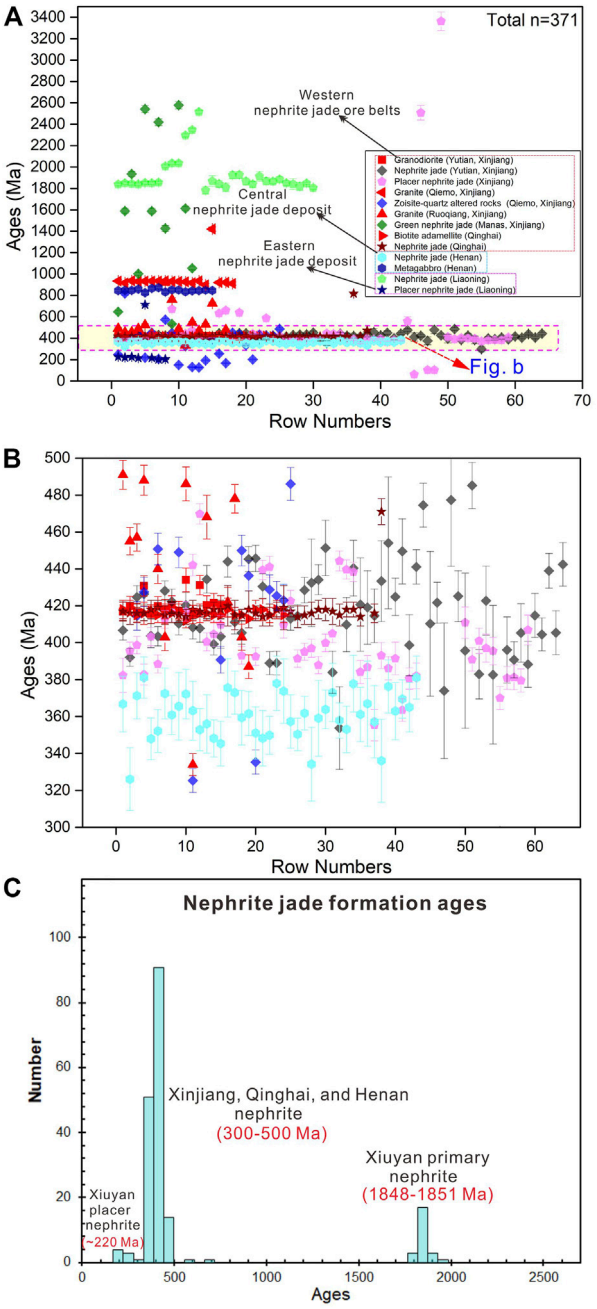

FIGURE 6
Geochronological data of nephrite jade in China. **(A)** Combined with the wide distribution of ages, it can be seen that chronological studies on nephrite jade are mainly concentrated in the Xinjiang regions, with geochronological investigations in other regions being more lacking and information in the southern region being in a state of absence. Overall, the formation ages from different provenances reveal the multi-period characteristics of nephrite jade mineralization in China. **(B)** The ages of nephrite deposit resources in China are mostly constrained at ~500–300 Ma. **(C)** Age data histogram of nephrite jade in China (Data cited by Liu et al., 2010; 2011; 2015; Ling et al., 2015; Liu et al., 2016; Lei et al., 2018; Gao et al., 2019; Zheng et al., 2019; Zou et al., 2021; Jiang et al., 2020). Due to the lack of effective dating data for nephrite jade deposits in the eastern and southern metallogenic belts, it is very limited to infer tectonic evolution mechanisms.

3.1.3.6 The Qinghai nephrite jade

In Qinghai Province, the jade mostly shows weak greasy-glass luster, semi-transparent-slightly transparent, and the overall transparency is higher than that nephrite jade from Xinjiang Province. The majority of jades in Qinghai Province are characterized by typical "waterline," and their economic value is far lower than that nephrite jade in Xinjiang Province (Figure 2D). The major nephrite jade deposits are hosted in Dazaohuo and Xiaozaohuo areas, Golmud City.

The main mineral of the Xiaozaohuo nephrite jade is tremolite (99%), with minor titanite and zircon (~1%). Almost all nephrite jade ores occur as vein, and a few nephrite jade ores even grew as pectinate, which indicates hydrothermal inputs (Lei et al., 2018). Published studies summarized that the Proto-Tethyan orogen in the east Kunlun region probably initiated in the early Cambrian, the subduction of its oceanic crust happened during the early Cambrian to early Silurian (515–438 Ma). Subsequently, the continental crust subduction and collision developed during the early to middle Silurian (436–425 Ma), and the post-collision was constrained in the late Silurian to the early Devonian (423–403 Ma) (Lei et al., 2018). Zircon U–Pb dating of the biotite adamellite indicates that the formation age of the Xiaozaohuo nephrite deposit was constrained at 416.4 ± 1.5 Ma, indicating tectonic correlation with post–collisional orogen of Proto-Tethyan Ocean in the eastern Kunlun region (Figure 6).

3.1.3.7 The Meiling nephrite jade

The jade (also termed as Meiling jade) deposit occurred in Liyang region, Jiangsu Province (Figure 1; Zhong, 1995; Cui and Yang, 2002; Li and Cai, 2008). The main mineral of the Meiling jade is tremolite, which also contains minor diopside, muscovite, epidote, apatite, magnetite, limonite, and clay minerals. The Meiling jade shows characteristics of low tremolite content, good orientation of tremolite fiber, and high crystallinity (Zhou et al., 2009).

3.2 Metamorphic-hydrothermal metasomatic nephrite jade deposits

These deposits were predominately discovered in the eastern nephrite jade metallogenic belt and the southern margin of North China Craton. Base on the characteristics of hydrothermal fluids and protoliths, the genetic type could be involved following two sections: serpentinite type and carbonate type (Liu and Yu, 2009). Most of orebodies which appears in veined and irregular shapes, controlled by multi-stage fault-fold structures.

3.2.1 The serpentinite type

The jade deposit is mainly hosted in the Fengtian and Wanrong areas of Hualien County, Taiwan Province, and the orebodies were embedded into ultramafic serpentinites (Lin, 1999; Ren et al., 2012). The nephrite jade orebodies were formed at the contact zones between the Paleozoic-Mesozoic Dananao schist and serpentinite. The lithologies of the exposed strata comprise mainly black pelitic schist, with minor green schists and mafic-ultramafic igneous rocks (Yui et al., 2014). The major minerals are characterized by fibrous tremolite with a subordinate association of actinolite, chromite, Cr-bearing garnet, magnetite, titanite, serpentine, chlorite, and graphite (Ren et al., 2012; Yui et al., 2014). The H-O stable isotopic data show that the $\delta^{18}D_{H2O}$ values range from −46.5‰ to −17.9‰, while the $\delta^{18}O_{H2O}$ values range from 5.2‰ to 6.0‰, respectively (Figure 5; Zhang, 2020). This type of nephrite jade deposits also have similar characteristics with the S-type nephrite jade deposits that generated in the ophiolite suites/belts.

3.2.2 The carbonate type

The nephrite jade orebodies usually occurred within the magnesium carbonate bodies and the hydrothermal fluid were mainly derived from the surrounding rocks where metamorphism occurs. Representative nephrite jade deposits are mainly distributed in Xiuyan of Liaoning, Luanchuan of Henan. Details are as follows.

3.2.2.1 The Xiuyan nephrite jade

These orebodies were developed in the structural fracture zones of tremolite dolomitic marble within the Dashiqiao Formation (Proterozoic Liaohe Group), Xiuyan County, Liaoning Province (Xu et al., 2000; Duan and Wang, 2002; Wang et al., 2002; Liu, 2013). The nephrite jade deposits generally underwent four stages: 1) dolomite deposition stage, 2) dolomite regional metamorphism stage, 3) hydrothermal metasomatism stage, and 4) weathering (Duan and Wang, 2002). The main mineral of nephrite jade is tremolite, characterized by SiO_2 contents more than 60%. The MgO and CaO contents are slightly lower, and the secondary or accessory minerals consist of calcite, dolomite, titanite, zoisite, apatite, chromite, and graphite (Jiang, 2014; Wu et al., 2014; Zhang et al., 2019). Moreover, the Xiuyan nephrite jade shows depletion in LREEs (Duan and Wang, 2002; Zhang et al., 2019). The similar REEs distribution patterns and H-O stable isotopes ($\delta^{18}D_{H2O}$: −73.3‰–−48.0‰; $\delta^{18}O_{H2O}$: 8.5‰–12.4‰) suggest that the Xiuyan nephrite jade deposit has close genetic correlation with dolomite marble.

3.2.2.2 The Luanchuan nephrite jade

The jade orebodies were developed in the conjugate areas of NE–and NW–trending faults (Yin, 2006; Ling et al., 2015). Most of the nephrite jade are hosted within serpentine jade or marble bodies, followed by altered gabbro veins or small compressive belts. White nephrite jade and dark green serpentine jade alternately occur as layers or veins, indicating typical epigenetic deposits (Figure 2H). The Luanchuan nephrite jade is characterized by tremolite with a subordinate association of dolomitic marble, serpentine, magnetite, and titanite. (Yin, 2006; Wang, 2013). Moreover, the nephrite jade has pronounced positive Eu anomalies, enriched light REE, and flat heavy REE (Yin, 2006; Ling et al., 2008) (Figure 4D). SIMS U–Pb dating of symbiosis titanite yielded lower intercept ages of 361 ± 4 Ma, constraining the formation timing of this jade deposit (Figure 6).

4 Formation mechanisms of nephrite jade deposits

4.1 Nephrite jade classification

Through the summarization the characteristics of nephrite jade in different regions of China, we can recognize that the two types of nephrites were formed in different tectonic geodynamic settings. The green nephrite jade was formed by the metasomatism of

serpentinite protolith (mainly antigorite) or by direct precipitation during orogeny (Zhang et al., 2021). Nephrite jade commonly presents green color, which is attributed to distinct contents of trace elements such as Fe^{2+}, Cr^{3+} (Yu et al., 2021; Zhang et al., 2021). In contrast, the nephrite jade after dolomitization is generally formed through skarn-type metasomatism between intermediate-felsic granitic rocks (granodiorites) and dolomite marbles (mainly from Xinjiang, China), suggesting a post-collision geodynamic setting (Gao et al., 2019; Zhang et al., 2022). High-quality nephrite jade presents white color, generally depending on constituent minerals or Fe trace elements. Accordingly, the distributions of nephrite jade deposits in China are predominantly related to serpentinites (S-type) and carbonate rocks (D-type), or being re-defined as green jade-type (GJ-type) and white jade-type (WJ-type), respectively.

4.2 Metallogenic mechanisms of GJ-type nephrite jade

As summarized above, the GJ-type nephrite deposits are hosted mainly in the north of Kunlun Mountains, the North Qilian orogenic belt, the west margin uplift zone of Yangtze Craton, and the South China Sea plate.

The GJ-type nephrite jade generated in Manas, Qilian, as well as Shimian, are quite similar in terms of tectonic settings and metallogenic processes (Figure 1). Previous investigations suggested that the formation of the Manas GJ-type nephrite jade deposit was related to ultramafic rocks and may have been formed by regional metamorphism of ultramafic magmatic rocks (Yang et al., 2012; Tian, 2014), or it was possibly transformed by serpentine to GJ-type nephrite through metasomatism, as shown in formula (Eqs 4-1-1, 4-1-2; Jiang et al., 2021).

$$3\,(Mg, Fe)_2SiO_4\ (Olivine) + 4H_2O + SiO_2 \rightarrow 2\,(Mg, Fe)_3Si_2O_5\,(OH)_4\ (Serpentine) \quad (4-1-1)$$

$$5\,(Mg, Fe)_3Si_2O_5\,(OH)_4\ (Serpentine) + 14SiO_2aq + 6CaO \rightarrow 3Ca_2\,(Mg, Fe)_5Si_8O_{22}\,(OH)_4\ (Tremolite - Actinolite) + 7H_2O \quad (4-1-2)$$

Zhang (2020) indicated that the Manas nephrite jade deposit originated in the ophiolitic mélange belt and was closely related to supra-subduction zone (SSZ) ophiolite (mantle wedge type ophiolite), suggesting that it was formed in a late subduction or post–subduction environment (Figures 7A, B). Moreover, the formation of tremolite may be linked to metamorphic diopside in two possible transformation modes (Zhang, 2020): 1) metasomatism; or 2) dissolution and precipitation. The presence of fluids may have led to the replacement of pre-existing diopside, which in turn may have facilitated the formation of tremolite. The detailed reaction formula is:

$$2CaMgSi_2O_6\ (Diopside) + 3MgOaq + 4SiO_2aq + H_2Ol = Ca_2Mg_5\,[Si_4O_{11}]_2\,(OH)_2\ (Tremolite/Actinolite) \quad (4-1-3)$$

However, the source or timing of introduction of Ca-rich fluids related to ultramafic rock type is a major concern that need to be addressed (Zhang et al., 2021). The Ca in the Manas nephrite jade deposit may have been derived from the surrounding mafic rocks (Zhang, 2020). The H-O stable isotope data suggest that the ore-forming fluids during the formation processes of green nephrite jade was derived from metamorphic water, implying the role of metamorphism (Zhang, 2020) (Figure 5). Zircon U–Pb dating data suggest the GJ-type nephrite jade is characterized by multi-stage metallogenic characteristics, and the formation ages should be no later than the Carboniferous ophiolite (Zhang, 2020) (Figure 6). Recently, we firstly investigated high-quality GJ-type nephrite (tremolite) jade from the Yushigou ophiolite suite, Qilian orogeny, NW China, which provides insight into the tectonic processes associated with the formation of jade within subduction zone settings (Yu et al., 2021; Zhang et al., 2021). Zircon U–Pb dating of nephrite jade samples in Yushigou region shows the weighted average age of 227.9 ± 5.3 Ma, representing multiple fluid-rock interaction events within suprasubduction zone at mantle and the formation age of nephrite jade. Thus, we propose that the developed faults during North Qilian Orogeniss might have acted as a pathway for the transfer of Ca- or COH-rich fluids in mantle-derived magma and fluid-rock interactions in the convergent margin setting and further facilitated the crystallization of tremolite or actinolite (Zhang, 2019; Yu et al., 2021; Zhang et al., 2021) (Figures 7A–C).

However, the formation processes of the Hualien nephrite jade were characterized by late subduction of the South China Sea plate (Yui et al., 2014). Based on the Barros type metamorphic superposition associated with arc-continent collision, the metamorphic and metasomatic temperature data supported that the fluid-rock interaction may have occurred, which further suggest the formation of the Hualien nephrite jade was constrained in the Mesozoic or earlier subduction-accretion complexes (Yui et al., 2014). The O-H isotopic data suggested that the fluids during the formation of this nephrite jade was derived from metamorphic water (Figure 5). In addition, Yui et al. (2014) obtained the formation age of 3.3 ± 1.7 Ma through NanoSIMS in–situ zircon U–Pb dating on edge of zircons, indicating that the Hualien nephrite jade is the youngest nephrite jade exposed on the Earth surface. Moreover, according to the graphite Raman micro-thermometer, the formation temperatures of the Hualien nephrite jade may be constrained in the range of 410°C–430°C and infer that the Hualien nephrite jade possibly formed in a relatively low P/T environment (Ren et al., 2012; Yui et al., 2014). Although the nephrite ore bodies are discovered at contact zones with serpentinite and greenschist-facies (carbonaceous material -) quartz-mica schist (Liu and Yu, 2009; Li et al., 2011; Yui et al., 2014), it exhibits profound similarities to the GJ-type nephrite jade deposits mentioned above in terms of geotectonics.

Based on the research findings about the GJ-type nephrite jade deposits in Manas, Qilian, and Hualien, we argue that the following doubts could be addressed. 1) The ultramafic nephrite jade usually occurs in/near ophiolite or ophiolite mélange zones, which are formed in different environments. Serpentinization that occurred in a subduction slab and in an overlying mantle wedge obviously has different tectonic significance (Martin et al., 2020; Zhang et al., 2021). Therefore, the detailed metallogenic environments of the green nephrite jade still needs to be clarified further. 2) The Ca sources may have been derived from the natural fluid system released by subducted slabs and then migrated to higher levels

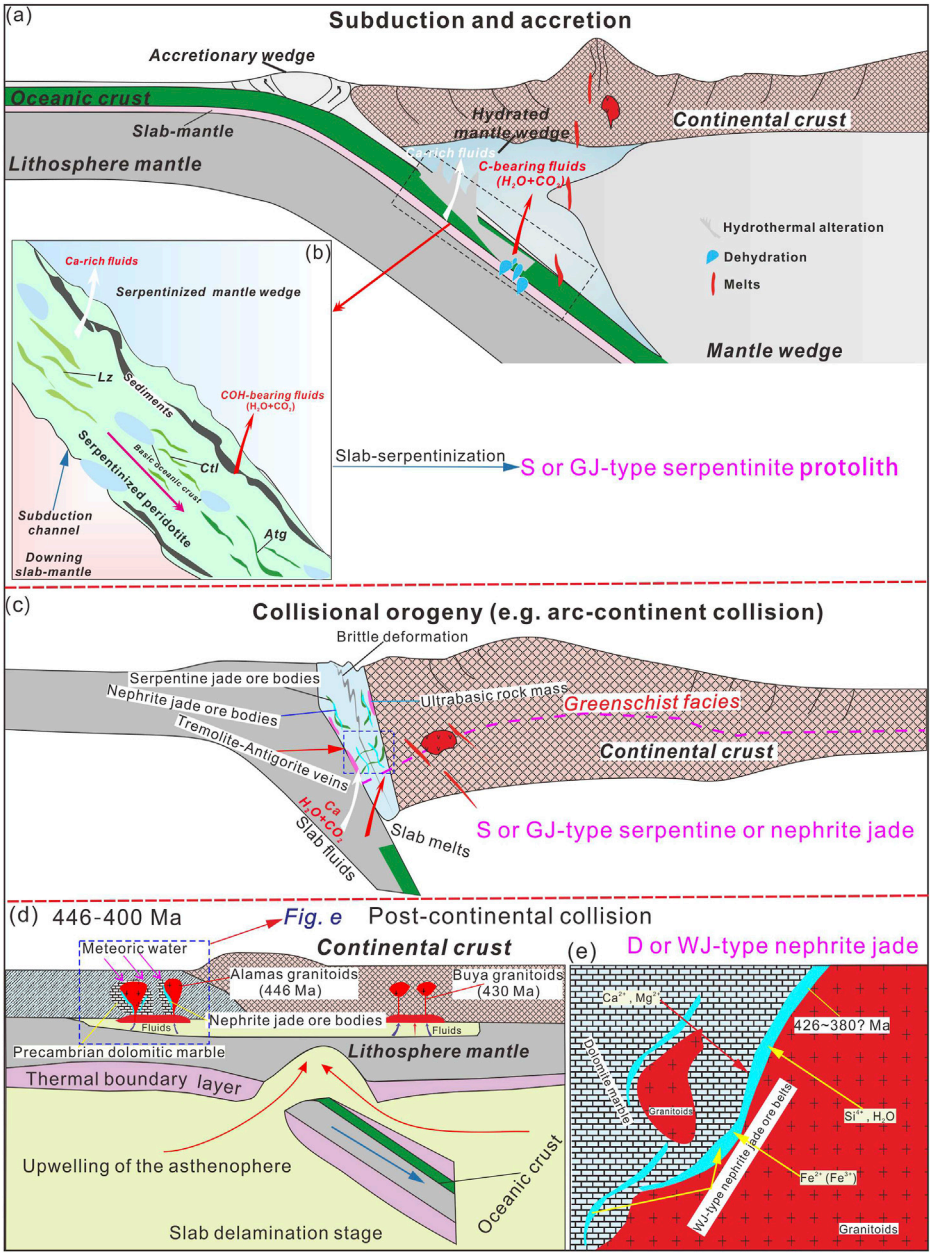

FIGURE 7
(A) Tectonic evolution of jade in initial subduction processes, during which only S or GJ-type primitive serpentinite was formed through the influx of slab derived fluids carrying Ca and CO_2 in the subduction zone (after Zhang et al., 2021). **(B)** Two serpentinization processes in the subducting slabs and overlying mantle wedge are envisaged, accompanied by the release of Ca and C-H-O fluids (Zhang et al., 2021). **(C)** Tectonic setting of jade in collision process, during which S or GJ-type nephrite jade was formed through the late auto-metamorphic metasomatism of serpentine or spontaneous crystallization/precipitation along suture/shear zones being Ca-rich fluids during orogeny at terrane or convergent margin settings in a cooling fore-arc environment (Cluzel et al., 2020; Zhang et al., 2021). **(D)** Post-collisional extension, coupled with limited asthenospheric upwelling, occurred at ~446 Ma (after Zhang et al., 2016). The evolution was accompanied by D-type or WJ-type nephrite jade formation through metamorphic metasomatism triggered by late orogenesis. **(E)** The formation mechanism pattern of D-type or WJ-type nephrite jade ore belts or veins, formed by direct contact between granitoids and marbles. Note that this model also applies to nephrite jade deposits associated with mafic rock types. These two sketches are not to scale. Abbreviations: Lz, Lizardite, Chl, Chrysotile, Atg, Antigorite.

through fluid channels or pathways (Zhang et al., 2021) (Figures 7B, C). 3) Single zircon U–Pb dating data may hardly constrain the metallogenic age of green nephrite jade, but when combined with the characteristics of zircon trace elements, it may provide useful suggestion about its formation and evolution (Zhang et al., 2021). The U–Pb age dating of symbiosis apatite or titanite may serve as reliable constraint for the formation age of green nephrite jade deposits considering their closure temperatures. 4) Research on nephrite mineralization mechanism in the Shimian area is almost non-existent, and so it is urgent to solve ore genesis and carry out

comparative investigations with other appraisal areas. Therefore, although previous researchers have carried out lots of investigations on GJ-type nephrite jade deposits in China (e.g., Yui et al., 2014; Zhang, 2020; Zhang et al., 2021), several issues remain regarding to their ore genesis, occurrence settings, and formation ages, which need to be addressed in further work.

4.3 Metallogenic mechanisms for WJ-type nephrite jade

In the western Hetian Nephrite Belt, representative primary (e.g., Alamas, Tashsaii, and Yinggelike) and secondary nephrite deposits (White Jade River and Black Jade River) in the Xinjiang Province, show high degree of consistency in terms of REEs distribution patterns, H-O isotopes, and information ages, implying similar metallogenic mechanisms (Figures 4–6). Specially, the H-O isotope data of the nephrite jade indicate that the water during nephrite jade formation was derived from metamorphic and magmatic water, as well as minor meteoric water (Figure 5). Whereas the primary nephrite jade deposits are divided into two stages, with the first stage of prograde metasomatism and the second stage of early retrograde alteration (Liu et al., 2011; 2015; 2016; Gao et al., 2019; Jiang et al., 2021). Previous investigations of petrological observations and mineral compositions revealed that WJ-type nephrite jade in Xinjiang underwent two metasomatism-metamorphism processes (Liu et al., 2011; 2015; 2016): 1) dolomite marble → tremolite; or 2) dolomite marble → diopside → tremolite. The principal formation models of primary deposits can be interpreted by the following equilibrium formulas (Eqs 4-2-1–4-2-3), which are consistent with the genetic model (Eq. 4-2-4) proposed by Harlow and Sorensen (2005):

$$5CaMg(CO_3)_2\ \text{(Dolomitic marble)} + 8SiO_2aq + H_2O \rightarrow Ca_2Mg_5[Si_4O_{11}]_2(OH)_2\ \text{(Tremolite)} + 3CaCO_3\ \text{(Calcite)} + 7CO_2aq \quad (4-2-1)$$

$$CaMg(CO_3)_2\ \text{(Dolomitic marble)} + 2SiO_2aq \rightarrow CaMg(Si_2O_6)\ \text{(Diopside)} + 2CO_2aq \quad (4-2-2)$$

$$5CaMg(Si_2O_6)\ \text{(Diopside)} + H_2O \rightarrow Ca_2Mg_5[Si_4O_{11}]_2(OH)_2\ \text{(Tremolite)} + 3Ca^{2+} + 6SiO_2 \quad (4-2-3)$$

$$5Ca(Mg,Fe)(CO_3)_2\ \text{(Dolomitic marble)} + 8SiO_2aq + H_2O \rightarrow Ca_2(Mg,Fe)_5[Si_4O_{11}]_2(OH)_2\ \text{(Tremolite}-\text{Actinolite)} + 3CaCO_3\ \text{(Calcite)} + 7CO_2aq \quad (4-2-4)$$

$$7CaMg(CO_3)_2\ \text{(Dolomitic marble)} + 3Fe^{2+} + 16SiO_2aq + 2H_2O \rightarrow 2Ca_2(Mg,Fe)_5[Si_4O_{11}]_2(OH)_2\ \text{(Tremolite)} + 3Ca^{2+} + 14CO_2aq \quad (4-2-5)$$

Actually, the reaction (Eq. 4-2-4) is applicable to the formation process of green to black jade because it can account for the provenance of Fe sources. However, the green to black WJ-type nephrite jade in China was attributed to a metasomatized dolomite origin due to their low Ni and Cr contents, and is enriched in Fe and Mn as well (Douglas, 1996), suggesting that those components existed either in the protolith of this jade or in the composition of post-magmatic or metasomatizing fluids (Douglas, 1996; 2003; Harlow and Sorensen, 2005). Therefore, the equation (Eq. 4-2-5) proposed by Gao et al. (2019) should be taken into account for the metallogenic process of the WJ-type nephrite in China. Recently, Zhang et al. (2022) proposed that the Fe absorption of epidote-altered diopsidite had a positive impact on the formation of high-quality nephrite jade, which providing new implications for the formation and evolution of the Saidikulam nephrite deposit. In contrast, more complicated formation processes were revealed by placer/secondary nephrite jade deposits, as demonstrated by Liu et al. (2011, 2016), with the presence of abundant mineral associations and metasomatic textures, and therefore, the formation reactions should be the integrated by the comprehensive equations (Eqs 4-2-2, 4-2-3) and (Eqs 4-2-6, 4-2-7):

$$CaMg(CO_3)_2\ \text{(Dolomitic marble)} + 2SiO_2aq \rightarrow Ca_2FeAl_2(SiO_4)(Si_2O_7)O(OH)_2\ \text{(Epidote)} + 2CO_2aq \quad (4-2-6)$$

$$Ca_2FeAl_2(SiO_4)(Si_2O_7)O(OH)_2\ \text{(Epidote)} \rightarrow Ca_2Mg_5[Si_4O_{11}]_2\ \text{(Tremolite)} \quad (4-2-7)$$

The nephrite jade deposits in Qinghai area of the Eastern Kunlun Orogen are commonly attributed to magmatic–hydrothermal deposits (Lei et al., 2018) except for several nephrite deposits combined with distinct igneous intrusive rocks (e.g., Sanchakou), whose formation processes can also be represented by reactions of Eqs 4-2-1–4-2-3.

In the eastern nephrite jade metallogenic belt, nephrite jade deposits (except Liyang, Jiangsu Province) are broadly distributed along the Jiao-Liao-Ji belt, the only generally accepted Paleoproterozoic orogenic belt in the Sino-Korean craton in the western Pacific Ocean (Xu and Liu, 2019; Zhang et al., 2019). The Tieli and Panshi nephrite jade deposits in Heilongjiang and Jilin Provinces, respectively, show similar formation mechanisms although their REEs distribution patterns show distinct characteristics (Figure 4E), which also suggest that the ore-forming fluids had multiple sources with differing characteristics and mineralization occurred as a multi-stage superposition process (Gao et al., 2019; Bai et al., 2020). Previous investigations proposed that the two-stage geological processes for the formation of the Tieli and Panshi nephrite ore bodies included an earlier contact metasomatism and a subsequent tremolitization and diopsidization of dolomitic marble during intrusion of intermediate-felsic intrusive rocks (granitoids) and magmatic hydrothermal metasomatism (Gao et al., 2019; Bai et al., 2020). Recently, Xu and Bai (2022) argued that the subduction of the Pacific Plate may have supplied source materials and power for magmatism and mineralization in the Tieli nephrite deposit based on the $^{87}Sr/^{86}Sr$ isotopic signatures in apatite, which links the subduction-related metasomatism-metamorphism and mineralization events in the circle-Pacific area. The Liyang nephrite (Meiling jade) orebody occurs in the external contact zones where Yanshanian (Jurassic-Cretaceous) Miaoxi granite and Paleozoic Permian Qixia Formation magnesium carbonate facies are discovered (Zhong, 1995; Cui and

Yang, 2002; Li and Cai, 2008), and its formation processes has higher similarity to that of the Tieli and Panshi nephrite deposits. However, significant controversy has arisen regarding to the specific metallogenic model of the Sangpiyu nephrite jade in Xiuyan, Liaoning Province. Wu et al. (2014) suggested that the Sangpiyu nephrite jade deposit was metamorphic–hydrothermal carbonate type based on ^{30}Si stable isotope and REEs distribution patterns that are consistent with the REEs distribution models of the Xinjiang nephrite jade (Figures 4A, F). However, Zhang et al. (2019) argued that the actual hydrothermal fluid metasomatism contained minor Ca during formation of the Sangpiyu nephrite jade. The dolomite was metasomatized by Si-rich hydrothermal fluids to form serpentine, if the contents of Ca are slightly higher, it would be replaced by Si-rich hydrothermal fluids to form tremolite (Zhang et al., 2019). The relevant reactions are (Eq. 4-2-1) and (Eq. 4-2-8):

$$6CaMg[CO_3]_2\ (\text{Dolomitic marble}) + 4SiO_2aq + 4H_2O \rightarrow Mg_6[Si_4O_{10}](OH)_8\ (\text{Serpentine}) + 6CaCO_3\ (\text{Calcite}) + 6CO_2aq \quad (4-2-8)$$

Moreover, Zhang et al. (2019) constrained the formation temperature of graphite inclusions in different types of Sangpiyu nephrite jade samples using graphite Raman microthermometer. This indicates that the graphite inclusions were formed either in high temperature metamorphic facies or low temperature metamorphic facies (Zhang and Yu, 2018; Zhang et al., 2019). The SIMS zircon and titanite U-Pb geochronological data were acquired with ^{207}Pb/^{206}Pb ages of 1924.8 ± 8.3 Ma and 1848 ± 17 Ma (Zou et al., 2021) (Figure 6), respectively, which imply that the Sangpiyu nephrite jade was formed in the dolomite during the period of Paleoproterozoic regional metamorphism along the Jiao–Liao–Ji Belt ca. 2.2–1.9 Ga (Zhang et al., 2019). Notably, Zheng et al. (2019) proposed that the placer nephrite jade (D-type) from Xiuyan region was formed after 220.8 ± 7.6 Ma based on SRIMP zircon U–Pb analysis (Figure 6), which was not derived from primary deposit. Considering the widespread distribution of Mesozoic granites in this area, the relationship between the formation of the Xiuyan nephrite jade and the tectonic settings needs to be further investigated.

In the southern nephrite jade metallogenic belt, the mineralization processes of the Luodian jade and the Dahua jade are related to the contact metamorphism between mafic rocks (diabase) and carbonate rocks (limestone or dolomitic limestone), but they differ significantly in the distribution patterns of REEs, which indicate differences in geological evolution (Figure 4D). The REEs data indicate that the Luodian jade is homologous with diabase and limestone, but its REE patterns are closer to those of limestone, suggesting interactions between the limestone and gas-liquid fluid during the mineralization (Figure 4D). Based on the calculation of ^{18}O fractionation equation between the tremolite and ore-forming fluids, the Luodian jade is classified as a medium-low temperature hydrothermal deposit (Yang, 2013). Accordingly, we argue that the Luodian jade was not produced by contact metasomatism of a single diabase intrusion, but the interactions between the diabase and carbonate. In addition, it was also attested that the bidirectional replenishment model of calcium and magnesium from mafic magma promoted the formation of the Luodian jade (Yang, 2013). For example, the common δEu and δCe exhibit significant negative anomalies in the Luodian jade, indicating that mineralization formed under a relatively reduced environment. However, the significant differences of REEs in the Dahua nephrite jade show multiple sources and the multi-stage superposition of mineralization by ore-forming fluids (Figure 4D; Yin, 2006; Ling et al., 2015). Previous investigation revealed that the mean value of ^{87}Sr/^{86}Sr of the Dahua jade is 0.7071, which is between limestone and diabase, further indicating that close linkages in the sources of ore-forming materials (Lan, 2022). Despite their formation ages and tectonic evolution are not well constrained, their formation processes could be characterized by reactions of Eqs 4-2-1–4-2-3.

4.4 Tectonic implications and prospecting potential of nephrite jade

From the perspective of geotectonic contexts, the formation of GJ-type and WJ-type nephrite deposits was being closely linked to subduction- collision- orogeny processes (Figure 7). Previous investigation indicates that the ophiolites are fragments of on-land oceanic, back-arc, and arc lithosphere, representing arc-continent collisions, or appearing to be isolated bodies that have ramped up upon (obducted onto) continental margins (Harlow and Sorensen, 2005). The tectonic environment for GJ-type is thought to have occurred under this context. Serpentinization during initial subduction provided the necessary serpentinite protolith for the formation of GJ-type nephrite jade in later period, and the evolutionary processes were accompanied by the migration of Ca and the variation of δ^{57}Fe isotopes (Figures 7A, B; Gil, et al., 2020; Zhang et al., 2021). The GJ-type nephrite jade deposits were then formed in the stage of metamorphic metasomatism processes of serpentine induced by the arc-continental collision in response to multiple fluid–rock interactions in mantle of suprasubduction zones (Figure 7C; Yui et al., 2014; Yang et al., 2017; Zhang et al., 2021). In contrast, previous investigations proved that the WJ-type nephrite jade deposits were mostly formed during post continent–continent collision, such as the Kunlun orogenic belt containing ~1,300 km nephrite jade metallogenic belt (Zhang et al., 2016; Lei et al., 2018; Gao et al., 2019) (Figure 1; Figures 7D, E). While the WJ-type nephrite jade deposits near the Pacific orogenic belt may be closely coupled with metamorphism–metasomatism triggered by the subduction of the western Pacific plate.

As the major nephrite jade deposits in China, the geotectonic background of the complex ophiolite suite/ophiolitic mélange belt or the ultramafic serpentine body represents the main prospecting destination for green nephrite jade. The GJ-type nephrite jade associated with ophiolite suites/belts or ultramafic serpentinites in China is presumably even more significant, which should necessitate enhanced investigations and excavation in the future. Further, the contact zones between intermediate-felsic/mafic intrusive rocks and carbonate bodies or sides of carbonate bodies may offer prospecting directions for white nephrite jade or white-green nephrite jade, which mainly depend on the sources of the hydrothermal fluids.

5 Concluding remarks

The integrated geological settings, gemological and mineralogical properties, geochronology, REEs, as well as H-O isotopes data from nephrite jade deposits in China allow us to draw the following preliminary conclusions:

1. The major nephrite jade deposits in China are divided into the western nephrite jade metallogenic belt, the eastern nephrite jade metallogenic belt on the west coast of the Pacific Ocean, the southern nephrite jade metallogenic belt, and the central nephrite jade metallogenic belt at the southern margin of North China Craton. The genetic types of nephrite jade are also defined as GJ-type and WJ-type.
2. The GJ-type nephrite deposits were formed through the late auto-metamorphic metasomatism of serpentine or spontaneous crystallization along suture/shear zones during late orogeny. The WJ-type nephrite jade ore bodies are generally hosted in the contact zones of dolomitic marbles and intermediate-felsic rocks or mafic rocks, which was formed through metamorphism-metasomatism processes during post continent-continent collision.
3. The formation of nephrite jade in China has been linked to the actions of hydrothermal fluids dominantly caused by metamorphic and magmatic sources, characterized by multi-stage metallogenic events.

Author contributions

Conceptualization, CZ, FY, XY, and EC; Methodology, CZ, JC, and PZ; Writing—original draft preparation, all authors; Writing—review and editing, CZ, FY, and EC; Supervision, CZ and FY; Funding acquisition, FY and CZ. All authors have read and agreed to the submitted version of the manuscript.

Funding

This research was jointly supported by the National Natural Science Foundation of China (Grant No. 42202077), the Natural Science Foundation of Gansu Province (Grant No. 22JR5RA440), the Fundamental Research Funds for the Central Universities (Grant No. LZUJBKY-2022-42), the talent research start-up fund of Qilu University of Technology (Shandong Academy of Sciences), and the Guiding Special Funds of "Double First-Class (First-Class University and First-Class Disciplines)" (Grant No. 561119201) of Lanzhou University, China.

Acknowledgments

We are grateful to Ms. Min Zhang (the first author's wife), Dr. Zhengyu Long (China University of Geosciences, Beijing), Ms. Shiyu Ma (Hebei GEO University), and Mr. Lu Niu, Ms. Yanan Bi and Mr. Mingzhe Chen from Qilu University of Technology for their help during data summary and collection. The Mr. Yu Wu (Gemological Inspection Institute of Zhongjian, Xinjiang) is appreciated for his generous sharing of precious placer nephrite jade samples. In addition, we also thank Prof. Jianjun Li (NGDTC) for identifying Luanchuan nephrite jade through FTIR and Dr. Ying Jiang (Jinling Institute of Technology) for providing field investigation figures related to D-type nephrite jade deposits.

Conflict of interest

The authors declare that the research was conducted in the absence of any commercial or financial relationships that could be construed as a potential conflict of interest.

Publisher's note

References

Adamo, I., and Bocchio, R. (2013). Nephrite jade from val malenco, Italy: Review and update. *Gems Gemology* 49 (2), 98–106. doi:10.5741/gems.49.2.98

Adams, C. J., Beck, R. J., and Campbell, H. J. (2007). Characterisation and origin of New Zealand nephrite jade using its strontium isotopic signature. *Lithos* 97 (3), 307–322. doi:10.1016/j.lithos.2007.01.001

Bai, F., Du, J. M., Li, J.-J., and Jiang, B. H. (2020). Mineralogy, geochemistry, and petrogenesis of green nephrite from Dahua, Guangxi, Southern China. *Ore Geol. Rev.* 118, 103362. doi:10.1016/j.oregeorev.2020.103362

Bai, F., Li, G. M., Lei, J. L., and Sun, J. X. (2019). Mineralogy, geochemistry, and petrogenesis of nephrite from Panshi, Jilin, northeast China. *Ore Geol. Rev.* 115, 103171. doi:10.1016/j.oregeorev.2019.103171

Che, Y. D. (2013). *Gemology and Mineralogy study on Luodian nephrite. Master thesis*. Beijing, China: China University of Geosciences. (in Chinese with English Abstract).

Chen, Q. L., Bao, D. Q., and Yin, Z. W. (2013). Study on XRD and infrared spectroscopy of nephrites from Xinjiang and xiuyan. *Liaoning. Spectrosc. Spectr. Analysis* 33 (11), 3142–3146. (in Chinese with English Abstract).

Cluzel, D., Boulvais, P., Iseppi, M., Lahondère, D., LesimpleetMaurizot, S., Paquette, J. L., et al. (2020). Slab-derived origin of tremolite–antigorite veins in a supra-subduction ophiolite: The peridotite nappe (New Caledonia) as a case study. *Int. J. Earth Sci.* 109, 171–196. doi:10.1007/s00531-019-01796-6

Cui, W. Y., and Yang, F. X. (2002). Study on Hetian jade (tremolite jade). *Acta Petrologica Mineralogica* 21 (1), 26–23. (in Chinese with English Abstract).

Ding, Y. (2011). Brief discussion on comparison and market prospect of Longxi nephrite and nephrite cat's-eye in Sichuan Province. *J. Graduate Sun Yat-sen Univ. Nat. Sci. Med.* 32 (02), 79–84. (in Chinese with English Abstract).

Dong, J. W., Wang, Y. Q., Qiu, C. J., Wang, J. W., and Huang, Y. X. (2014). Mineralogy characteristics of Guizhou nephrite. *J. East China Univ. Sci. Technol. Nat. Sci. Ed.* 4 (60), 713–717. (in Chinese with English Abstract).

Douglas, J. G. (2003). "Exploring issues of geological source for jade worked by ancient Chinese cultures with the aid of X-ray fluorescence," in *Scientific study in the field of Asian art*. Editor P. Jett (London, UK: Archetype Publications Ltd.), 192–199.

Douglas, J. G. (1996). The study of Chinese archaic jades using non-destructive X-ray fluorescence spectroscopy. *Acta Geol. Taiwanica* 32, 43–54.

Du, J. M. (2015). *The study on gemological and mineralogical characteristics of nephrite in Dahua, Guangxi. Master thesis*. Beijing, China: China University of Geosciences. (in Chinese with English Abstract).

Duan, T. Y., and Wang, S. L. (2002). Study on stable isotopes of Xiuyan nephrite (tremolite). *Acta Petrologica Mineralogica* 21 (1), 115–119. (in Chinese with English Abstract).

Fang, T. (2018). Characteristics and cause of formation of Gobi nephrite from southern Xinjiang. *J. Gems Gemmology* 20 (05), 27–38. (in Chinese with English Abstract).

Feng, X. Y., and Zhang, B. L. (2004). Study on compositions and texture characteristics of nephrite from Qinghai province. *J. Gems Gemmology* 6 (4), 7–9.

Feng, Y. H., He, X. M., and Jing, Y. T. (2022). A new model for the formation of nephrite deposits: A case study of the chuncheon nephrite deposit, South Korea. *Lithos* 141, 104655. doi:10.1016/j.oregeorev.2021.104655

Gao, K., Fang, T., Lu, T. J., Lan, Y., Zhang, Y., Wang, Y. Y., et al. (2020). Hydrogen and oxygen stable isotope ratios of dolomite-related nephrite: Relevance for its geographic origin and geological significance. *Gems Gemmology* 56 (2), 266–280. doi:10.5741/gems.56.2.266

Gao, K., Shi, G. H., Wang, M. L., Xie, G., Wang, J., Zhang, X. C., et al.(2019). The tashisayi nephrite deposit from south Altyn Tagh, Xinjiang, northwest China. *Geosci. Front.* 10 (4), 1597–1612. doi:10.1016/j.gsf.2018.10.008

Gao, S. J. (2014). *Master thesis*. Beijing, China: China University of Geosciences. (in Chinese with English Abstract).The study on gemological and mineralogical characteristics and Genesis of nephrite in Tieli Heilongjiang

Gil, G., Bagiński, B., Gunia, P., Madej, S., Sachanbiński, M., Jokubauskas, P., et al. (2020). Comparative Fe and Sr isotope study of nephrite deposits hosted in dolomitic marbles and serpentinites from the Sudetes, SW Poland: Implications for Fe-As-Au-bearing skarn formation and post-obduction evolution of the oceanic lithosphere. *Ore Geol. Rev.* 118, 103335. doi:10.1016/j.oregeorev.2020.103335

Han, D., Liu, X. F., Liu, Y., Zhang, Y., Zheng, F., Maituohuti, A., et al. (2018). Genesis of dolomite-related nephrite from Hetian and color-forming factors of typical nephrite in Hetian, Xinjiang. *Acta Petrologica Mineralogica* 37 (6), 1011–1026. (in Chinese with English Abstract).

Harlow, G. E., and Sorensen, S. S. (2005). Jade (nephrite and jadeitite) and serpentinite: Metasomatic connections. *Int. Geol. Rev.* 47 (2), 113–146. doi:10.2747/0020-6814.47.2.113

Harlow, G. E., and Sorensen, S. S. (2000). *31st international geologic congress*. Rio de JaneiroAbstracts: Congress Program, 72. Brazil, August 6-17, 2000.Jade: Occurrence and metasomatic origin [abs

Harlow, G. E., Sorensen, S. S., Sisson, V. B., and Shi, G. (2014). "Chapter 10: The Geology of jade deposits," in *The Geology of gem deposits. Short course handbook series 44*. Editor Lee A. Groat 2nd Edition (Quebec: Mineralogical Association of Canada), 305–374.

Jiang, B. H., Bai, F., and Zhao, J. K. (2021). Mineralogical and geochemical characteristics of green nephrite from Kutcho, northern British Columbia, Canada. *lithos* 399-389, 106030. doi:10.1016/j.lithos.2021.106030

Jiang, T. L. (2014). *The study on gemological and mineralogical characteristics of nephrite in Sangpiyu, liaoning province. Master thesis*. Beijing, China: China University of Geosciences. (in Chinese with English Abstract).

Jiang, Y., Shi, G. H., Xu, L. G., and li, X. L. (2020). Mineralogy and geochemistry of nephrite jade from Yinggelike deposit, Altyn Tagh (Xinjiang, NW China). *Minerals* 10 (5), 418. doi:10.3390/min10050418

Jiang, Y. (2020). *Study on petro-mineral features and genetic mechanism of Ruoqiang nephrite, Xinjiang province. PhD thesis*. Beijing, China: China University of Geosciences. (in Chinese with English Abstract).

Kim, W. S. (2007). Addressing disparities in access to oral health care in Canada. *Can. Gemmol.* 4 (28), 119–124. doi:10.53581/jopv.2022.4.1.119

Lan, Y. (2022). *Geochemical characteristics and genesis of tremolite jade in Dahua, Guangxi. Master thesis*. Gunagxi: Guilin University of Technology. (in Chinese with English Abstract).

Lei, C., Yang, M. X., and Zhong, Z. Q. (2018). Zircon U–Pb ages and Hf isotopes of the Xiaozaohuo nephrite, eastern Kunlun orogenic belt: Constraints on its ore-forming age. *Geotect. Metallogenia* 42 (1), 108–125. (in Chinese with English Abstract).

Li, H. J., and Cai, Y. T. (2008). Study on characteristics of nephrite from Liyang, Jiangsu province. *J. Gems Gemmology* (03), 16–19. (in Chinese with English Abstract).

Li, J. (2016). *PhD thesis*. China: China University of Geosciences Wuhan. (in Chinese with English Abstract).Mineralogical and gemological characteristics of typical nephrites in China for the origin identification on Liangzhu ancient jades

Li, X., Zhang, C., Behrens, H., and Holtz, F. (2020). Calculating amphibole formula from electron microprobe analysis data using a machine learning method based on principal components regression. *Lithos* 362-363, 105469. doi:10.1016/j.lithos.2020.105469

Li, Y. Z., Liao, G. L., and Zhi, Y. X. (2011). Microstructure and vibration spectrum study of Nephrite from Taiwan. *Acta Petrologica Mineralogica*, 73–77. (in Chinese with English Abstract).

Liao, G. L., Zhou, Z. Y., and Liao, Z. T. (2012). XRD and IR spectra study on green nephrite from taiwan. *J. Gems Gemmology* 14 (04), 23–29. (in Chinese with English Abstract).

Liao, R. Q., and Zhu, Q. W. (2005). Chemical composition analyses of nephrite from all Chinese locations in China. *J. Gems Gemmology* 1 (07), 25–30. (in Chinese with English abstract).

Lin, S. S. (1999). Varieties and characteristics of nephrite (amphibole jade) from taiwan province. *J. Gems Gemmology* (03), 18–20. (in Chinese with English Abstract).

Ling, X. X., Schmädicke, E., Qiu, L.-L., Gose, J., Wu, R. H., Wang, S. Q., et al. (2015). Age determination of nephrite by *in-situ* SIMS U–Pb dating syngenetic titanite: A case study of the nephrite deposit from luanchuan, henan, China. *Lithos* 220-223, 289–299. doi:10.1016/j.lithos.2015.02.019

Ling, X. X., Wu, R. H., Bai, F., Yin, J. N., and Li, W.-W. (2008). A study of tremolite jade from Luanchuan, Henan Province. *Acta Petrologica Mineralogica* 27 (2), 157–163. (in Chinese with English Abstract).

Liu, F., and Yu, X. Y. (2009). Types of deposits and mineralogical characteristics of nephrite in China. *Mineral Resour. Geol.* 23 (04), 375–380. (in Chinese with English abstract).

Liu, X. F., Jia, Y. H., and Liu, Y. (2019). Geochemical characteristics and genetic types of Gobi nephrite in ruoqiang-qiemo, Xinjiang. *Rock Mineral Analysis* 38 (03), 316–325. (in Chinese with English Abstract).

Liu, Y., Deng, J., Shi, G. H., Lu, T. J., He, H. Y., Ng, Y. N., et al. (2010). Chemical zone of nephrite in Alamas, Xinjiang, China. *Resour. Geol.* 60 (3), 249–259. doi:10.1111/j.1751-3928.2010.00135.x

Liu, Y., Deng, J., Shi, G. H., Sun, X., and Yang, L. (2011a). Geochemistry and petrogenesis of placer nephrite from hetian, Xinjiang, northwest China. *Ore Geol. Rev.* 41 (01), 122–132. doi:10.1016/j.oregeorev.2011.07.004

Liu, Y., Deng, J., Shi, G. H., Yu, T. F., Zhang, G., Abuduwayiti, M., et al. (2011b). Geochemistry and petrology of nephrite from Alamas, Xinjiang, NW China. *J. Asian Earth Sci.* 42 (03), 440–451. doi:10.1016/j.jseaes.2011.05.012

Liu, Y. F. (2013). *Metallogenic regularity and prospecting indicator of the jade deposit in the Xiuyan area, liaoning province*. Master thesis. Jilin: Jilin University. (in Chinese with English Abstract).

Liu, Y., He, M. Y., Maituohuti, A., and Shi, G. H. (2011). Genesis of the nephrite from Alamas in hetian, Xinjiang. *Acta Petrologica Mineralogica* 30, 39–46. (in Chinese with English Abstract).

Liu, Y., Zhang, R. Q., Abuduwayiti, M., Wang, C., Zhang, S. P., Shen, C. H., et al. (2016). SHRIMP U–Pb zircon ages, mineral compositions and geochemistry of placer nephrite in the Yurungkash and Karakash River deposits, West Kunlun, Xinjiang, northwest China: Implication for a Magnesium Skarn. *Ore Geol. Rev.* 72, 699–727. doi:10.1016/j.oregeorev.2015.08.023

Liu, Y., Zhang, R., Zhang, Z., Shi, G. H., Zhang, Q., Anuduwayiti, M., et al. (2015). Mineral inclusions and SHRIMP U–Pb dating of zircons from the Alamas nephrite and granodiorite: Implications for the Genesis of a magnesian skarn deposit. *Lithos* 212–215, 128–144. doi:10.1016/j.lithos.2014.11.002

Lu, B. Q., Qi, L. J., Xia, Y. B., and Zhou, K. C. (2004). Mineralogy of nephrite (tremolite) cat's eye from Sichuan Province. *Acta Petrologica Mineralogica* (03), 268–272. (in Chinese with English Abstract).

Lu, B. Q., Qi, L. J., and Xia, Y. B. (2007). Raman spectra of nephrite cat's eye and the relationship between Raman spectra and the cat's eye colors. *J. Chin. Ceram. Soc.* (11), 1492–1494. (in Chinese with English Abstract).

Lu, B. Q., Qi, L. J., and Xia, Y. B. (2008). Study on the vibration spectra of nephrite cat's eye from Sichuan Province. *Shanghai Geol.* (03), 57–60. (in Chinese with English Abstract).

Lu, B. Q. (2005). *The gemological mineralogy and spectroscopy nephrite cat's eye sichuan, sichuan province, southwest China*. PhD thesis. Shanghai: Shanghai University. (in Chinese with English Abstract).

Ma, D. R. (2013). *Characteristics and metallogenic law of the Sanchakou jade ore in Golmud, Qinghai. Master thesis*. Beijing: China University of Geosciences. (in Chinese with English abstract).

Martin, C., Flores, K. E., Vitale-Brovaroned, A., Angiboustf, S., and Harlow, G. E. (2020). Deep mantle serpentinization in subduction zones: Insight from *in situ* B isotopes in slab and mantle wedge serpentinites. *Chem. Geol.* 545, 119637. doi:10.1016/j.chemgeo.2020.119637

McDonough, W. F., and Sun, S. S. (1995). The composition of the Earth. *Chem. Geol.* 120 (3), 223–253. doi:10.1016/0009-2541(94)00140-4

Meng, Y. (2014). *The causes and genesis study of nephrite in Alamas Yutian Xinjiang China*. Master thesis. Beijing, China: China University of Geosciences. (in Chinese with English Abstract).

Qin, Y. (2013). *Study on gemological Characteristics and mineral components of Qinghai black Nephrite*. Master thesis. Beijing, China: China University of Geosciences. (in Chinese with English Abstract).

Qiu, K. F., Goldfarb, R. J., Deng, J., Yu, H. C., Gou, Z. Y., Ding, Z. J., et al. (2020). Gold deposits of the jiaodong peninsula, eastern China. *Seg. Spec. Publ.* 23, 753–773.

Qiu, L. (2016). *Gemological study of nephrite gravel*. Master thesis. Beijing, China: China University of Geosciences. (in Chinese with English Abstract).

Ren, S. M., Zhang, L. J., and Zhang, J. (2012). Mineral composition, microstructure characteristics and generation of taiwan nephrite. *J. Guilin Univ. Technol.* 32 (1), 36–42. (in Chinese with English Abstract).

Song, H. L., Tan, H. L., and Zu, E. D. (2020). Spectral characteristics of Qinghai nephrite with different colors. *Bull. Chin. Ceram. Soc.* 39 (01), 242–246. (in Chinese with English Abstract).

Su, Y., Yang, M. X., Wang, Y. Y., Chang, Y. Y., and Li, Y. (2019). Gemological characteristics of Gobi nephrite from southern Xinjiang, China. *J. Gems Gemmology* 21 (04), 1–10. (in Chinese with English Abstract).

Tang, Y. L., Liu, D. Q., and Zhou, R. H. (2002). Geological characteristics of Manasi green jade in Xinjiang. *Acta Petrologica Mineralogica* 21 (1), 22–25. (in Chinese with English Abstract).

Taylor, H. P., Jr. (1997). "Oxygen and hydrogen isotope relationships in hydrothermal mineral deposits," in *Geochemistry of hydrothermal ore deposits*. Editor H. L. Barnes 3rd ed. (New York: Wiley-Interscience), 229–302.

Tian, S. (2014). *Gemological characteristics and mineral typomorphic characteristics of green Xinjiang manasi nephrite*. Master thesis. Hebei: Shijiazhuang University of Economics. (in Chinese with English Abstract).

Wang, B. Y., Chen, H., and Zhang, Y. (2017). *Mineralogical and gemological characteristics of green nephrite from linwu, hunan province, China*. International Gem and Jewelry Academic Conference. (in Chinese with English Abstract).

Wang, F. (2016). *Black nephrite's characteristics and preliminary study of graphite's influence on its quality. Master thesis*. Xinjiang: Xinjiang University. (in Chinese with English Abstract).

Wang, S. B. (2013). Study on mineralogy and metallogenic temperature of luanchuan nephrite in henan province zhao. *Public Sci. Technol.* 15 (12), 82–84. (in Chinese with English Abstract).

Wang, S. Q., Duan, T. Y., and Zheng, Z. Z. (2002). Mineralogical and petrological characteristics of Xiuyan nephrite and its minerogenetic model. *Acta Petrologica Mineralogica* 21 (1), 79–90. (in Chinese with English Abstract).

Wu, L. J. (2016). *Study on gemological and mineralogical characteristics and genesis of nephrite in Tiantai, Qiemo, Xinjiang. Master thesis*. Beijing, China: China University of Geosciences. (in Chinese with English Abstract).

Wu, Z. Y., Wang, S. Q., and Ling, X. X. (2014). Characteristics and origin of nephrite from Sangpiyu, xiuyan country, liaoning province. *Acta Petrologica Mineralogica* 33 (2), 15–24. (in Chinese with English Abstract).

Xu, H. P., Feng, A. P., Wang, S. Q., Zhu, W. J., and Deng, W. (2000). The origin of Liaoning Xiuyan nephrite placer resources and their protection. *Resour. Sci.* 22 (2), 24–29. (in Chinese with English Abstract).

Xu, H. S., and Bai, F. (2022). Origin of the subduction-related Tieli nephrite deposit in Northeast China: Constraints from halogens, trace elements, and Sr isotopes in apatite group minerals. *Ore Geol. Rev.* 142, 104702. doi:10.1016/j.oregeorev.2022.104702

Xu, L. G., Yu, X. J., and Wang, S. Q. (2014). The gemological characteristics and origin of Donggang Village tremolite jade in Dahua,Guangxi. *Acta Petrologica Mineralogica* (1), 55–60. (in Chinese with English Abstract).

Xu, W., and Liu, F. L. (2019). Geochronological and geochemical insights into the tectonic evolution of the paleoproterozoic jiao-liao-ji belt, Sino-Korean craton. *Earth-Science Rev.* 193, 162–198. doi:10.1016/j.earscirev.2019.04.019

Xu, Y. X., Lu, B. Q., and Qi, L. J. (2015). A petromineralogical and SEM microstructural analysis of nephrite in Sichuan Province. *Shanghai Land and Resour.* 36 (03), 87–89. (in Chinese with English Abstract).

Yang, F., Santosh, M., Tsunogae, T., Tang, L., and Teng, X. M. (2017). Multiple magmatism in an evolving suprasubduction zone mantle wedge: The case of the composite mafic–ultramafic complex of Gaositai, North China Craton. *Lithos* 284-285, 525–544. doi:10.1016/j.lithos.2017.05.004

Yang, J., Zhang, Y. F., Qiu, Z. L., Jia, D. L., and Zheng, X. Y. (2021). Geochemistry and petrogenesis of greenstone belt type serpentine jade from taishan, shandong. *Geotect. Metallogenia* 45 (05), 1044–1059. (in Chinese with English abstract).

Yang, L., Lin, J. H., Wang, L., Wang, B., and Du, Y. (2013). IR spectrum characteristics and significance of luodian jade from Guizhou. *Spectrosc. Spectr. Analysis* 33 (8), 2087–2091. (in Chinese with English Abstract).

Yang, L. (2013). *Study on petro-mineral features and genetic mechanism of luodian jade, Guizhou province. PhD thesis*. Sichuan: Chengdu University of Technology. (in Chinese with English Abstract).

Yang, X. D., Shi, G. H., and Liu, Y. (2012). Vibrational spectra of black species of hetian nephrite (tremolite jade) and its color genesis. *Spectrosc. Spectr. Analysis* 32 (3), 681–685. (in Chinese with English Abstract).

Yin, J. N. (2006). *Petrology and deposit research on nephrite and serpentine of luan chuan, henan province abstract. Master thesis*. Beijing, China: China University of Geosciences. (in Chinese with English Abstract).

Yin, Z., Jiang, C., Santosh, M., Chen, Y. M., Bao, Y., and Chen, Q. L. (2014). Nephrite jade from Guangxi province, China. *Gems Gemology* 50 (3), 228–235. doi:10.5741/gems.50.3.228

Yu, H. Y. (2016). *Coloring and metallogenic mechanisms of different colors in Qinghai nephrite. PhD thesis*. Jiangsu: Nanjing University.

Yu, X. Y. (2016). *Colored gemmology*. 2nd Edition. BeijingBeijing, China: Geology Press, 236–244. (in Chinese).

Yu, X. Y., Long, Z. Y., Zhang, Y., Qi, L. J., Zhang, C., Xie, Z. R., et al. (2021). Overview of gemstone resources in China. *Crystals* 11 (10), 1189. doi:10.3390/cryst11101189

Yui, T. F., Usuki, T., Chen, C. Y., Ishida, A., Sano, Y., Suga, K., et al. (2014). Dating thin zircon rims by NanoSIMS: The fengtien nephrite (taiwan) is the youngest jade on earth. *Int. Geol. Rev.* 56 (16), 1932–1944. doi:10.1080/00206814.2014.972994

Zhang, C., Yu, X. Y., and Jiang, T. L. (2019). Mineral association and graphite inclusions in nephrite jade from Liaoning, northeast China: Implications for metamorphic conditions and ore Genesis. *Geosci. Front.* 10 (2), 425–437. doi:10.1016/j.gsf.2018.02.009

Zhang, C., and Yu, X. Y. (2018). Spectral characteristic and origin identification of tremolite jade from Sangpiyu, liaoning province. *J. Gems Gemmology* 20 (S1), 41–53. (in Chinese with English Abstract).

Zhang, C., Yu, X. Y., Yang, F., Santosh, M., and Huo, D. (2021). Petrology and geochronology of the Yushigou nephrite jade from the North Qilian Orogen, NW China: Implications for subduction related processes. *Lithos* 380-381, 105894. doi:10.1016/j.lithos.2020.105894

Zhang, H. Q. (2019). *Gemology, mineralogy and trace element study on green nephrite from Qinghai province*. Master thesis. Beijing: China University of Geosciences. (in Chinese with English abstract).

Zhang, L. Q. (2013)., 20. Beijing, China: China University of Geosciences, 41–53. (in Chinese with English Abstract).The study on the characteristics of composition, structure and spectroscopy of the nephrite from Luodian*Guizhou Prov. Master thesis*S1

Zhang, Q. C., Liu, Y., Huang, H., Wu, Z. H., and Zhou, Q. (2016). Petrogenesis and tectonic implications of the high-K Alamas calc-alkaline granitoids at the northwestern margin of the Tibetan Plateau: Geochemical and Sr–Nd–Hf–O isotope constraints. *J. Asian Earth Sci.* 127, 137–151. doi:10.1016/j.jseaes.2016.05.026

Zhang, X. C., Shi, G. H., Zhang, X. M., and Gao, K. (2022). formation of the nephrite deposit with five mineral assemblage zones in the central western Kunlun Mountains, China. *J. Petrology* 63, egac117. doi:10.1093/petrology/egac117

Zhang, X. M. (2020). *Mineralogy and genesis of green nephrite in the western section of Manas region, Xinjiang. PhD thesis*. Beijing, China: China University of Geosciences. (in Chinese with English Abstract).

Zhang, Y. D. (2015). *Study on geologic-geochemical property and metallogenic regularity of nephritic ore in luodian county, Guizhou province*. Guizhou: Guizhou University. (in Chinese with English Abstract).

Zhang, Y. W., Liu, Y., Liu, T., and Muhetaer, Z. (2012). Vibrational spectra of hetian nephrite of Xinjiang. *Spectrosc. Spectr. Analysis* 32 (2), 398–401. (in Chinese with English Abstract).

Zhang, Z. W., Gan, F. X., and Cheng, H. S. (2011). PIXE analysis of nephrite minerals from different deposits. *Nucl. Instrum. Methods Phys. Res. B Beam Interact. Mater. Atoms* 269 (4), 460–465. doi:10.1016/j.nimb.2010.12.038

Zheng, F., Liu, Y., and Zhang, H. Q. (2019). The petrogeochemistry and zircon U–Pb age of nephrite placer deposit in xiuyan. *Liaoning, Rock Mineral Analysis* 38 (04), 438–448. (in Chinese with English Abstract).

Zhi, Y. X., Liao, G. L., Chen, Q., Li, Y. Z., and Zhou, Z. Y. (2011). Gemmological and mineralogical characteristics of nephrite from luodian, Guizhou province. *J. Gems Gemmology* 13 (4), 7–13. (in Chinese with English Abstract).

Zhong, H. B. (1995). The discovery of meiling jade in south Liyang,Jiangsu. *Geol. Jiangsu* 19 (3), 176–178. (in Chinese with English Abstract).

Zhong, Q., Liao, Z. T., Qi, L. J., and Zhou, Z. Y. (2019). Black nephrite jade from Guangxi, southern China. *Gems Gemology* 55 (2), 198–215. doi:10.5741/gems.55.2.198

Zhou, Z. Y., Chen, Y., Liao, Z. T., and Y, Y. (2009). A petrological and mineralogical study of Liyang nephrite. *Rock Mineral Analysis* 28 (05), 490–494. (in Chinese with English Abstract).

Zhou, Z. Y., Liao, Z. T., Chen, Y., Li, Y. J., and Ma, T.-T. (2008). Petrological and mineralogical characteristics of Qinghai nephrite. *Rock Mineral Analysis* (01), 17–20. (in Chinese with English Abstract).

Zhou, Z. Y., Liao, Z. T., Ma, T. T., and Yuan, Y. (2005). Study on ore-forming type and genetic mechanism of Sanchakou nephrite deposit in Qinghai province. *J. Tongji Univ. Nat. Sci.* (09), 1191–1194+1200. (in Chinese with English Abstract).

Zou, T. R., Guo, L. H., Li, W. H., and Duan, Y. R. (2002). A study on Raman spectra of Hetian jade, Manasi green jade and Xiuyan old jade. *Acta Petrolocgica Mineralogica* (S1), 72–78. (in Chinese with English Abstract).

Zou, Y., Li, P., Wu, Z. Y., Kang, M. L., and Wang, S. Q. (2021). A study of the mineralization age of nephrite from Sangpiyu, xiuyan count, liaoning province. *Acta Petrologica Mineralogica* 40 (4), 825–834. (in Chinese with English abstract).